NASA/CR–2008–214163

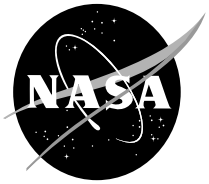

DC/DC Converter Stability Testing Study

Bright L. Wang

July 2008

The NASA STI Program Office … in Profile

Since its founding, NASA has been dedicated to the advancement of aeronautics and space science. The NASA Scientific and Technical Information (STI) Program Office plays a key part in helping NASA maintain this important role.

The NASA STI Program Office is operated by Langley Research Center, the lead center for NASA's scientific and technical information. The NASA STI Program Office provides access to the NASA STI Database, the largest collection of aeronautical and space science STI in the world. The Program Office is also NASA's institutional mechanism for disseminating the results of its research and development activities. These results are published by NASA in the NASA STI Report Series, which includes the following report types:

- TECHNICAL PUBLICATION. Reports of completed research or a major significant phase of research that present the results of NASA programs and include extensive data or theoretical analysis. Includes compilations of significant scientific and technical data and information deemed to be of continuing reference value. NASA's counterpart of peer-reviewed formal professional papers but has less stringent limitations on manuscript length and extent of graphic presentations.
- TECHNICAL MEMORANDUM. Scientific and technical findings that are preliminary or of specialized interest, e.g., quick release reports, working papers, and bibliographies that contain minimal annotation. Does not contain extensive analysis.
- CONTRACTOR REPORT. Scientific and technical findings by NASA-sponsored contractors and grantees.
- CONFERENCE PUBLICATION. Collected papers from scientific and technical conferences, symposia, seminars, or other meetings sponsored or cosponsored by NASA.
- SPECIAL PUBLICATION. Scientific, technical, or historical information from NASA programs, projects, and mission, often concerned with subjects having substantial public interest.
- TECHNICAL TRANSLATION. English-language translations of foreign scientific and technical material pertinent to NASA's mission.

Specialized services that complement the STI Program Office's diverse offerings include creating custom thesauri, building customized databases, organizing and publishing research results . . . even providing videos.

For more information about the NASA STI Program Office, see the following:

- Access the NASA STI Program Home Page at http://www.sti.nasa.gov/STI-homepage.html
- E-mail your question via the Internet to help@sti.nasa.gov
- Fax your question to the NASA Access Help Desk at (301) 621-0134
- Telephone the NASA Access Help Desk at (301) 621-0390
- Write to:
  NASA Access Help Desk
  NASA Center for AeroSpace Information
  7115 Standard Drive
  Hanover, MD 21076

NASA/CR–2008–214163

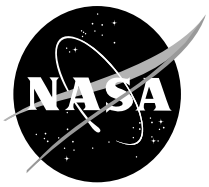

DC/DC Converter Stability Testing Study

Bright L. Wang
Perot Systems Government Services, Seabrook, Maryland

National Aeronautics and
Space Administration

Goddard Space Flight Center
Greenbelt, Maryland 20771

July 2008

Acknowledgments

The Author would like to thank Ashok K. Sharma for technical review and edit of the manuscript. The thanks also due to Jelila S. Mohammed, the Task Monitor; and Bruce D. Meinhold, the Task Lead; for their support throughout the project.

Available from:

NASA Center for AeroSpace Information
7115 Standard Drive
Hanover, MD 21076-1320

National Technical Information Service
5285 Port Royal Road
Springfield, VA 22161

TABLE OF CONTENTS

APPENDICES

1.0 INTRODUCTION

For the past several months, the Parts Analysis Laboratory of NASA Goddard Space Flight Center has been developing a test system that will allow the agency to inspect all flight DC/DC converters for electrical performance stability. Recent studies have shown that some system instability issues have the potential to cause catastrophic failures of DC/DC converters for NASA space flight missions [1] [2]. According to the studies, the failures including system oscillations have occurred 25 times between 1997 and 2001 during flight board functional tests, system level environmental tests, and space flight missions in several cases [3]. To ensure reliable flight electronic hardware for NASA future space exploration missions, it becomes critical to determine and evaluate stability conditions of the flight hybrid DC/DC converters during power system design and power subsystem level tests.

The stability test system consists of three measurement methods as follows: (1) impedance measurement, (2) gain/phase measurement, and (3) early detection of oscillation. This report describes the experimental study of utilizing these three methods to evaluate stability levels of the hybrid DC/DC converters. Such study is particularly important to continue further with the development of this test system, because the converters for space flight mission are very different from those open-frame converters that are batter suited for the commonly used gain/phase margin measurement techniques to determine their stability levels. Specifically, the new test system will apply the three test methods to component, board and system level tests for space grade hybrid DC/DC converters equiped with or without remote sense terminals.

The goal of this study was to find out whether the impedance measurement could help evaluate possibility of DC/DC converter front-end oscillation. Another objective was to determine how to perform gain/phase measurement on those hybrid DC/DC converters with and without remote sense terminals to evaluate possibility of feedback loop oscillation. In particular, the focus of this study was to understand relationship between input noise and feedback-loop oscillation by using signal analysis, in order to create a stability indicator which could represents gain/phase margins of hybrid DC/DC converters.

The study results indicated that the gain/phase measurement is an effective method to determine stability levels of hybrid DC/DC converters. Although, it is limited to those converters with remote sense terminals, it could be extended to testing lid-opened modules without remote sense pins during DPA processes, if a required test point for signal insertion can be located. The study also found that a channel power (in dBm) in a power spectrum of the converter input noise, at a frequency when phase angle of the feedback loop reaches 360°, apeared to be a reliable indicator for stability since the noise channel power level presented a high degree correlation with the gain/phase margins.

Beside above three findings, impedance measurement data from six DC/DC converter modules from three vendors showed that the line voltage and load current seemed to have significant effects on input impedance at low frequency range. Front-end oscillations found in all xxFL2800 modules are a clear evidence that a DC/DC converter with an unstable input impedance will be vulnerable to oscillations.

2.0 METHODS AND PROCEDURES

Three potential measurement techniques of the stability test system for DC/DC converters: impedance measurement, gain/phase margin measurement, and oscillation detection technique were experimentally studied using data processing and signal analysis methods. They are described in detial below.

2.1 Impedance Measurement for Front-End Oscillation

An earlier study on input impedance of switching-mode power converters was observed in 1971, when electro-magnetic interference (EMI) became a serious problem and input filters were required. Since then, numerous papers have been published to discuss the effect of adding input filter on power converters. An important conclusion from those studies stated that output impedance of the input filter should be much smaller than the input impedance of the power converter ($Z_s << Z_i$), otherwise the power converter could subject to a so-called front-end oscillation [4][5][6]. In fact, existence of this kind of oscillation has confirmed on several occasions during NASA flight hardware tests[1][2].

2.1.1 Input Impedance Varification Test

To verify if line voltage change (ΔV_{in}) and load change (ΔI_{out}) will result in input impedance ($Z_{in} = - R_{in}$) changes of NASA used hybrid DC/DC converters, and if so, how much the negative resistance changes are. Input impedances of three hybrid DC/DC converters from Interpoint, two from VPT, and one from International Rectifier (IR) were measured using a Ridley AP200 Frequency Response Analyzer. The measurement setup was established in NASA/GSFC Power System Branch (Code 563), and its block diagram is shown in Figure 1. For each of the six DC/DC converter modules, the input impedance data was collected at six different operating conditions, which include low, nominal, and high line voltages at zero, half and full load. An

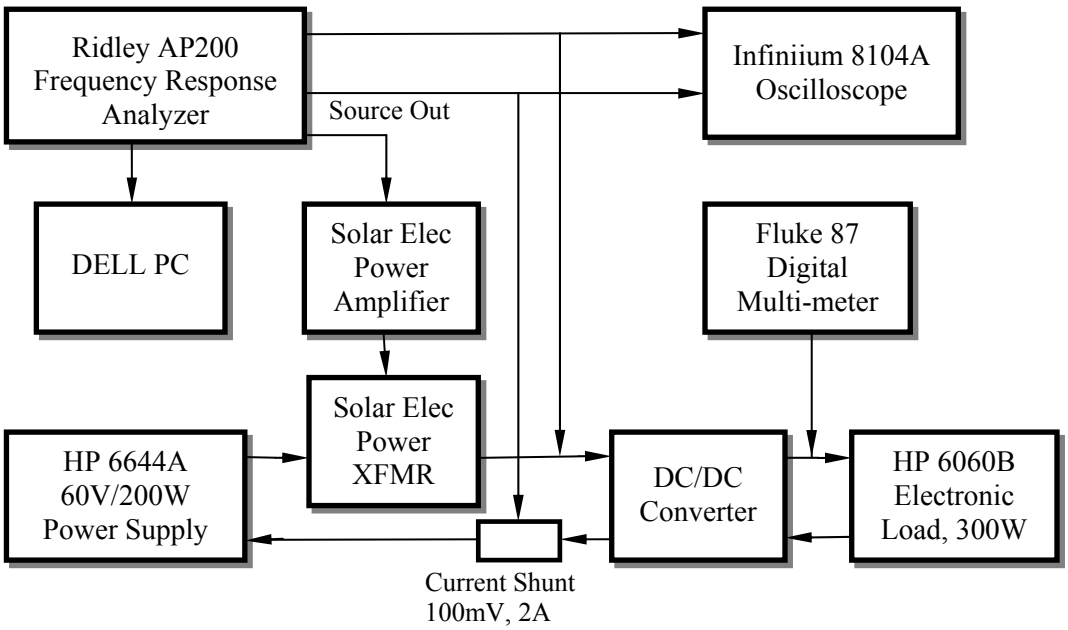

Figure 1: Input impedance measurement setup for DC/DC converters.

interaction signal of 200mV (≈1% of input voltage) was injected into the power input line through an injection transformer. All measurement data were generated in DAT file format by the Ridley AP200 frequency response analyzer. The data were later transferred to Excel spreadsheets for impedance-frequency curve generations.

2.1.2 Front-End Oscillation Observations

In order to understand how front-end oscillation is related to the input impedance of a DC/DC converter, an abnormal power source impedance was created by adding extra inductance into the input voltage line to alter the source impedance. A secondary winding of a Solar Electronic 6620-5A power transformer was used to simulate the extra inductance. Figure 2 shows the test setup to observe front-end oscillations. For three DC/DC converters, input voltage and output current were adjusted accordingly until the oscillation occurred and displayed on an oscilloscope. Then, maximum amplitude and frequency of the oscillation waveform, as well as the input voltage and current of the output were measured and recorded.

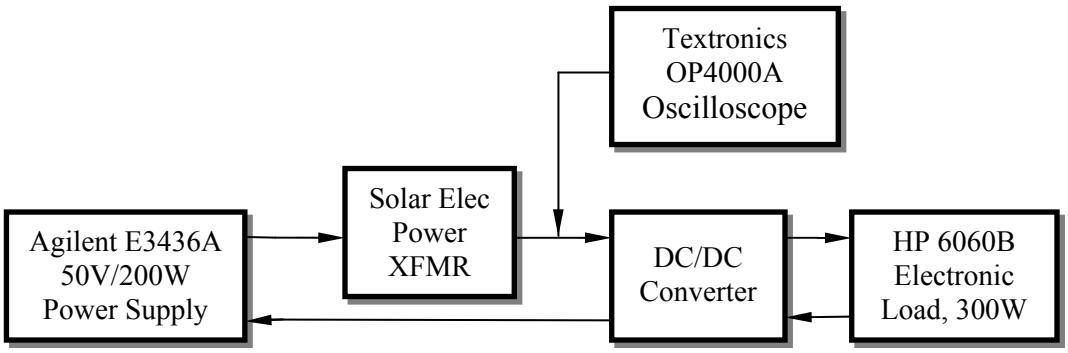

Figure 2: The test setup for observing front-end oscillation of DC/DC Converter

2.2 Gain/Phase Margin Measurement for Feedback Loop Oscillation

The feedback control loop of a hybrid DC/DC converter should be free of so-called feedback loop oscillation at any specified operating conditions to ensure a stable system operation. If the oscillation occurs, a DC/DC converter can be driven into an unstable situation and, in most cases, power transistors, output capacitors, and other parts of the converter can be instantly destroyed as the consequence. As a design "rule of thumb", a DC/DC converter must have a feedback loop gain less than unity (< 0 dB) when the feedback loop phase angle is a total of 360°, and the phase shift must be less than 360° when the gain around the loop is unity (= 0 dB), and the gain slope to pass crossover the unity gain must be -1 (20dB/decade). Thus, the only way to make the feedback loop stable at all required operating conditions is to maintain adequate safety margins for its loop gain and phase, and usually they are setup at least -15 dB for gain and 45° for phase shift [7].

Many studies have concluded that gain/phase margins are critical measures of DC/DC converter system stability. However, actual gain and phase margins for every individual hybrid DC/DC converter used in space flight projects are unknown. The fact is that a manufacturers' practice is to measure control loop gain/phase margins only on open-frame converter prototypes at a design stage to verify the designs, but not on final packaged products at post-production. One of the

reasons is that the measurement becomes nearly impossible due to probing difficulties, once the hybrid device is assembled and packaged. Another reason is that the manufacturers usually have high level of confidence about the gain/phase margins on their final products, although real test data may not there to support it.

To find a practical way to verify gain/phase margins by end users, some hybrid DC/DC converters were studied by accessing signal injection resistors through remote sense terminals and by opening the case lid. In addition, electrical and environmental effects on gain/phase margins were also studied. Figure 3(a) shows the gain/phase margin measurement setup using a Venable 3225 Frequency Response Analyzer. A typical Bode plot of the measurement is shown in 3(b). Notice that the parameter values of gain in dB, phase angle in Degree, and slope in 20dB per decade were used for this measurement.

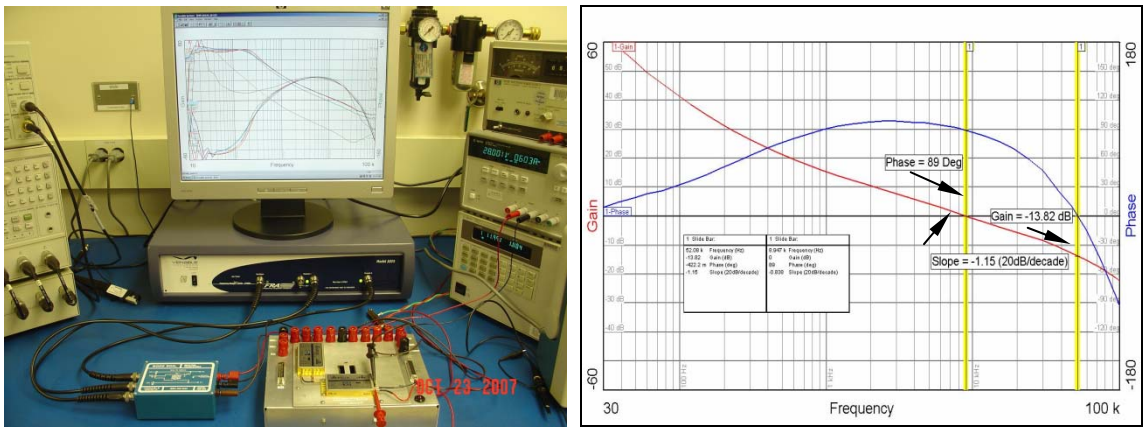

(a) (b)

Figure 3: Test configuration for Gain/phase margin measurement. (a) The test set up. (b) A typical Bode plot shown gain/phase margins and slope.

2.2.1 Using Remote Sense Terminal as Signal Injection Point

Measuring gain/phase margins requires access to a small value resistor to inject test signal into feedback loop. Some specific types of hybrid DC/DC converters that provided with a pair of terminals for output voltage remote sense or voltage adjustment are suitable for perform this measurement. For these types of modules, there is a small value resistor (10Ω to 200Ω) in series with control loop path on the circuit board, and it is connected between pins of voltage output (V_{out}) and positive sense (*Sense+*) or output adjustment (Adj.). With this resistor in place, a sine-wave signal at a swapped frequency range can be injected into the feedback loop and the gain/phase margins of the converter can be measured. Figure 4 shows the test method using remote sense terminals. By using this setup, a 100 kHz interaction signal generated from output (Out) of the Venable 3225 was injected into the feedback loop path through Venable 200 injection transformer output, V1 and V2. The internal small value resistor is in series with the feedback loop path and is connected to remote sense pin or output adjustment pin of the DC/DC converter module. However, this measurement method is accurate only if a DC/DC converter module has an internal resistor connected between voltage output (*Vout*) and positive sense (*Sense +*) terminals, and if the resistor value is between 10Ω and 200Ω. This is an essential requirement since many hybrid DC/DC converters ether do not have this resistor or do not have this range of values, even though they do have remote sense or output adjustment terminals.

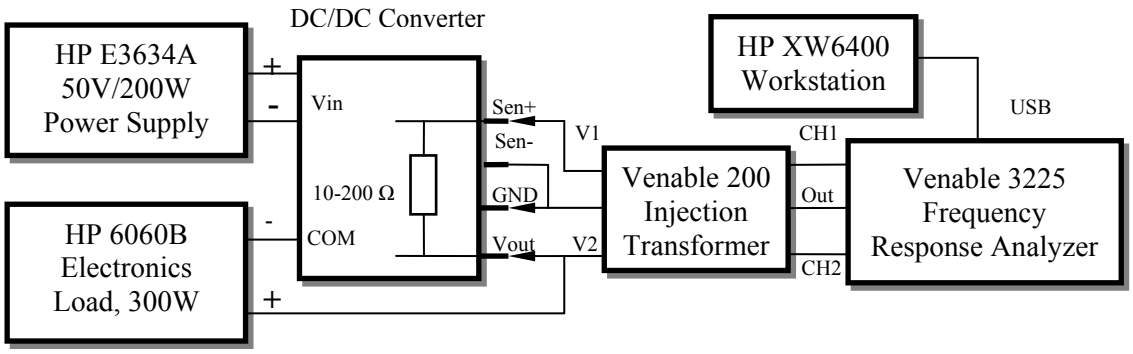

Figure 4: Test configuration for Gain/phase margin measurement through remote sense terminals connected with an internal 10 to 200-ohm resistor.

To determine which models of DC/DC converter meet the requirement for gain/phase margin measurement using remote sense terminals, some models equipped with or without remote sense or output adjustment pins from three vendors were evaluated. Table 1 lists the information gathered from this evaluation. One of the findings is that, in general, DC/DC converters with rated power below 15 watts do not provide either remote sense or output adjustment pins, and about 70% of the models from the three vendors are estimated to be less than 15 watts. Among the listed modules, MFL2800 and MTR2800 series from Interpoint, AFL2800 and ATW2800 series from IR, and DVFL2800 and DVTR2800 series from VPT have the internal resistor connected between *Vout* and *Sense+* terminals. However, the resistor values of Interpoint modules are too large to be used as the injection element, while IR and VPT's module seem to meet the requirement for injecting signal through the remote sense pins.

Table 1: Remote Sense or Output Adj. Pins Availability for Some Models.

Vendor	Model Series	Accessible Pins	Resistance, Pin V_{out} to Pin Sense+ or Adj.	Resistance, Pin V_{out} to Internal PWM
Interpoint	MFL2805S	Sense	6.7kΩ	216Ω+ a diode R
Interpoint	MFL2812S	Sense	11kΩ	216Ω+ a diode R
Interpoint	MSA2800	No	n/a	TBD
Interpoint	MCH2800	No	n/a	TBD
Interpoint	MHF2800	No	n/a	TBD
Interpoint	MTR2800	Sense	22kΩ	100Ω
IR	AFL2800	Sense	100Ω	n/a
IR	ASA2800	No	n/a	TBD
IR	ATR2800	Sense	TBD	n/a
IR	AHF2800	No	n/a	TBD
IR	M3G2800	No	n/a	TBD
IR	LS2800	Output Adj.	TBD	n/a
IR	ATW2800	Sense	100Ω	n/a
IR	ATS2800	Output Adj.	TBD	n/a
VPT	DVFL2800	Sense	30Ω	30Ω
VPT	DVHF2800	No	n/a	5.2kΩ
VPT	DVTR2800	Sense	100Ω	100Ω
VPT	DVWR2800	No	n/a	TBD

Based on the findings, three xxFL2800 series modules were chosen to study feasibility of utilizing remote sense pins as the test points to perform the gain/phase margin measurement. These three modules are rated from 65W to 100W, and are electrically and mechanically similar to Standard Microcircuit Drawing, SMD-5962-94721. The AFL2805S and DVFL2812S modules were tested by using the configuration of Figure 3, while the MFL2812S was connected a 20Ω external resistor between *Vout* and *Sen*+ Pin and was installed as shown in Figure 5. To keep the output voltage well regulated, the *Sen*- Pins were tied to the *COM* pin for both configurations.

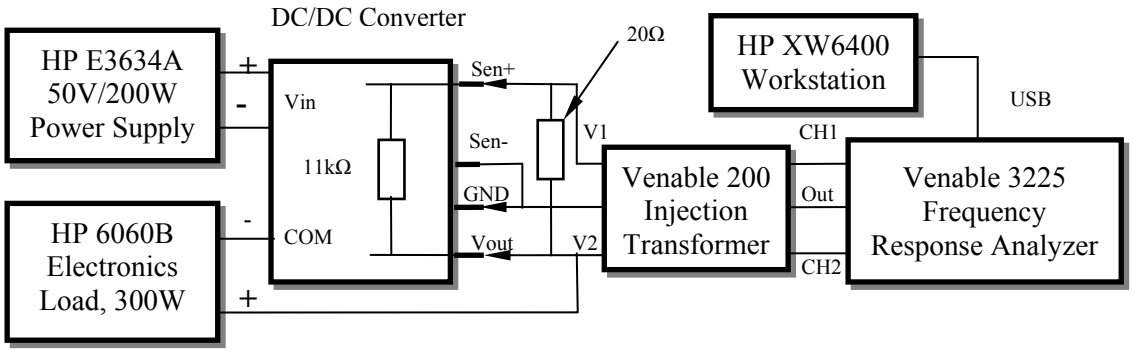

Figure 5: Test configuration for gain/phase margin measurement through remote sense terminals connected with an external 20Ω resistor.

2.2.2 Measuring Gain/Phase Margin on Open-lid Hybrid Modules

For hybrid DC/DC converters that do not have accessible remote sense pins, a gain/phase margin measurement could be performed if the module's top lid is removed. This study explored the possibility to run the measurement for certain type of the DC/DC converters, which could be used during destructive parts analysis (DPA) processes.

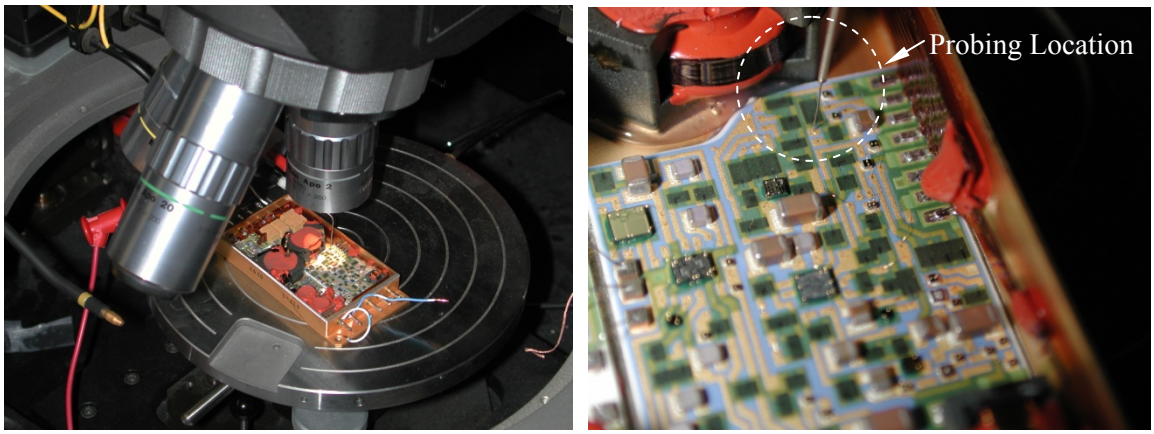

(a) (b)

Figure 6: Probing on the located signal injection resistor. (a) The SUSS probe setup, (b) A closer look at probing the resistors on board.

In order to develop this measurement method for DC/DC converters with lid opened, the signal injection resistor along the feedback loop path on the circuit board must be first located and identified. This will allow using a probe station as shown in Figure 6 to probe the resistor, and connecting a Venable 3225A analyzer to the resistor through probe tips. Figure 6 (b) shows a closer look at probing the resistor. Notice that all resistors in green color are embedded on an Aluminum-Nitride circuit board and are interconnected through gold-plated cooper traces. In this study, an Interpoint MFL2805S module was de-lidded, and several enlarged images that contain detailed circuit board construction and parts layout were obtained (see Figure 7). The injection resistor was traced down from the voltage output pin (*Vout*+) as an origin point until a resistor connected to the remote sense pin was found. Resistance value of this resistor was then measured using a multi-meter connected to the probe tips. For this MFL2812S module, a 216Ω resistor (R1) in series with a diode (D1) was found in connection between power output and remote sense pins. The diode was then bypassed using a micro-probe, and only the 216Ω resistor remained in active for noise rejection. Notice that the first solder pad in the upper left is the connection to the remote sense pin (*Sense*+), and the second one is connected to output positive pin (*Vout*+). The dark green area below the first solder pad is the 216Ω resistor with the D1 diode nears by.

A VPT DVHF2805S module was also de-lidded to find a possible point used to inject noise signal. This is the type of module that does not have remote sense terminals, so it can be a good

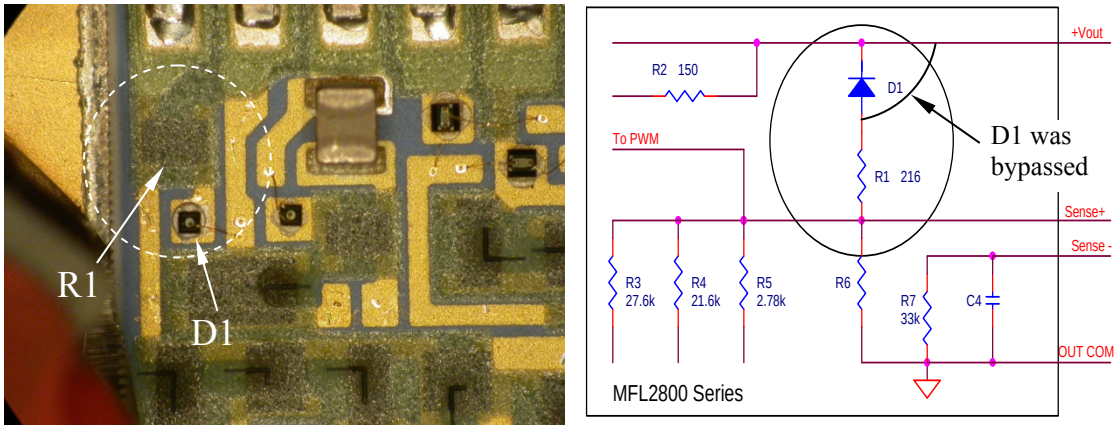

(a) (b)

Figure 7: Feedback loop resistor network of MFL2805S module. (a) Enlarged image shown the resistor R1. (b) Schematic derived from the circuit board layout.

example for using the open-lid measurement method. Several enlarged images that contain detailed circuit board construction and parts layout were obtained. Figure 8(a) and (b) present the images of feedback loop path and the injection resistor located using the same technique as described above. The derived schematic of the feedback loop section is provided in Figure 9 (a). As helpful information to end users, VPT's datasheet exclusively provides a schematic of the resistor network and *+Vout/ +Sense* terminals for DVFL2800 modules shown in Figure 9 (b). In fact, using R1 (30Ω) between *+Vout* and *+Sense* pins as the injection point has provided a convenient way to conduct the gain/ phase margin measurement, and this resistor was physically verified.

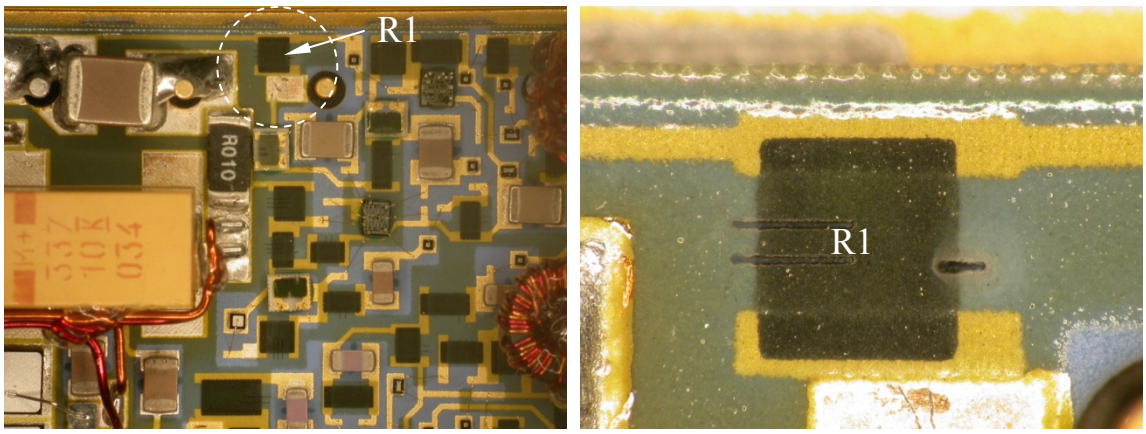

(a) (b)

Figure 8: (a) and (b), closer-look images of the feedback loop path and the resistor network of VPT DVHF2805S.

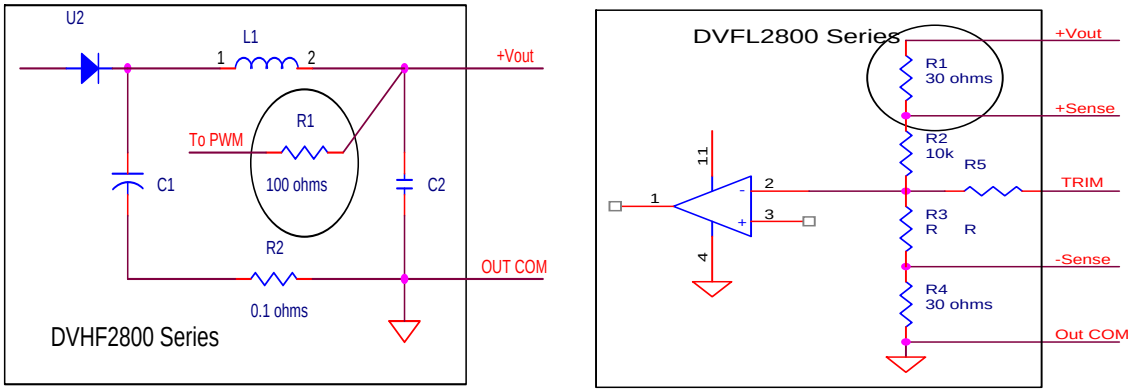

(a) (b)

Figure 9: Schematic of feedback loop path of (a) VPT DVHF2805S module, derived from the circuit board layout. (b) VPT DVFL2812S module, obtained from the vendor's datasheet.

2.2.3 Testing of Electrical and Environmental Effects on Gain/Phase Margins

Gain and phase margins of a DC/DC converter feedback loop are subject to change, if the electrical or environmental operation condition changes due to line voltage or load change, component electrical value change, and ambient temperature change. The feedback loop will oscillate if the gain/phase margin change to become too small and an external interference are introduced. To study how the gain/phase margins are affected by those factors, seven hybrid DC/DC converter modules, MFL2805S, MFL2812S, MTR2805S, AFL2805S, ATW2805S, DVFL2812S, and DVTR283R3S, and an open-frame module, QV24-5-25, were tested under several extreme operating conditions.

Load Current Effect Test This test was to verify the effects of load current changes on DC/DC converter feedback loop gain/phase margin. The gain/phase margins of the seven DC/DC converters were measured at a room temperature, while the load current of each module was changed from no-load to full-load in several intervals.

Base-plate Temperature Effect Test To study base-plate temperature effects on DC/DC converter feedback loop gain/phase margin, two modules, an AFL2805S and a DVFL2812S, were tested separately at the base-plate temperature of -55°C, 25°C and 125°C, using a *TPS Tenney-BTRC* environmental test chamber. Three line-voltages from low-line to high-line and three load currents from no-load to full-load were set to operate the modules at each of the three temperature settings. A temperature effect on converter switching frequency was also studied, using spectral analysis to measure the frequencies of the two modules.

Component Value Effect Test of Feedback Loop Compensation Network A stable DC/DC converter pulse-width-modulation (PWM) control process is realized by carefully designing input/output filters, feedback loop compensation network, and feedback loop sense network to set adequate zeros, poles and gain crossover frequency for the loop. This experiment was intentionally setup to obtain information on what kind of gain/phase margins could exist, if some critical part values of the feedback loop became inadequate to the circuit because of the part values drift, wrong parts used, and/or shortcomings in original design. An oscillation simulator shown in Figure 10(a) was designed and adopted to allow the feedback loop to oscillate when values of some compensation network parts were manually changed to deviate from their nominal values. A commercial QV24-5-25 open-frame DC/DC converter rated from 18V to 36V input and 5V/25A output was used for this simulator because of its easier part accessibility.

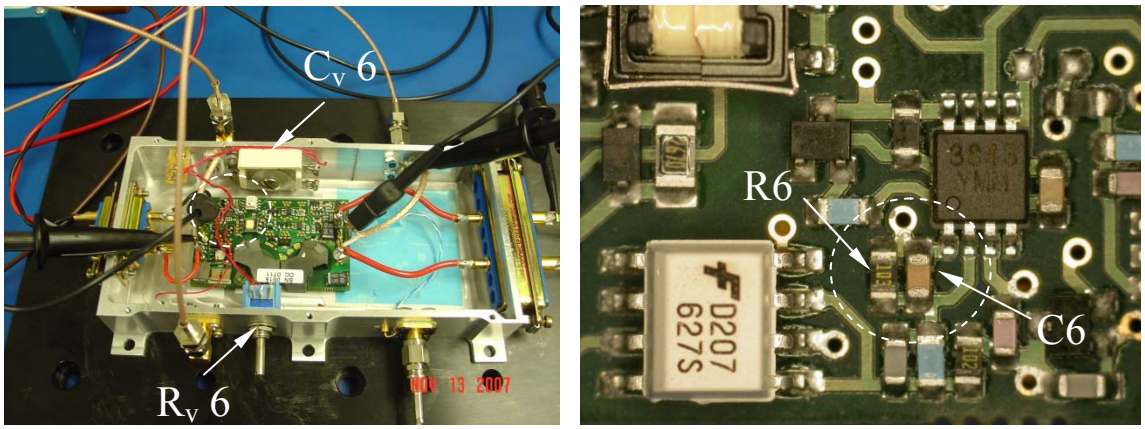

(a) (b)

Figure 10: (a) The feedback loop oscillation simulator, and (b) locations of R6 and C6 on board.

Figure 10(b) indicates the locations of the original resistor R6 (10kΩ) and capacitor C6 (3900pF), replaced then by a 10kΩ potentiometer, R_v6 and a 360pF variable capacitor, C_v6. A schematic of this simulator is show in Appendix A (a). By adjusting the R_v6 potentiometer gradually from 1kΩ to 10kΩ, this simulator was able to response in such a way that the oscillation development was stepwise from low level to very serious level. Several values of the R_v6 were preset, and Bode plots of the feedback loop response at each of the preset values were generated. Then, the gain/phase margins were measured accordingly.

2.3 Oscillation Identification and Early Detection

It has been determined that for hybrid DC/DC converters without remote sense terminals, directly measuring gain and phase margins using a frequency response analyzer becomes virtually impossible, and converters with no sense-pins are a majority among all families of various types. Therefore, an indirect method to estimate gain/phase margins could be a new approach for these converters with no sense pins provided. This new proposed approach was used to analyze input voltage noise, the only information obtainable for these type of converters. As a characterization study, a QV24-5-25 open-frame converter and three xxFL2800 series hybrid converters were tested for the noise level against its corresponding gain/phase margins. An Agilent N9320A spectrum analyzer was used to analyze the input voltage noise signal. This noise analysis system is shown in Figure 11(a). The 11(b) is a Fourier spectrum for QV24-5-25, showing the switching frequency fundamental in 306.5kHz mode and its harmonics. Figure 11(c) is an expected power spectrum of AFL2805S that contains a swiching fundamental frequency, and typically, an oscillation frequency. Figure (d) is a Bode plot showing gain and phase margins and the frequency that corresponds to the oscillation.

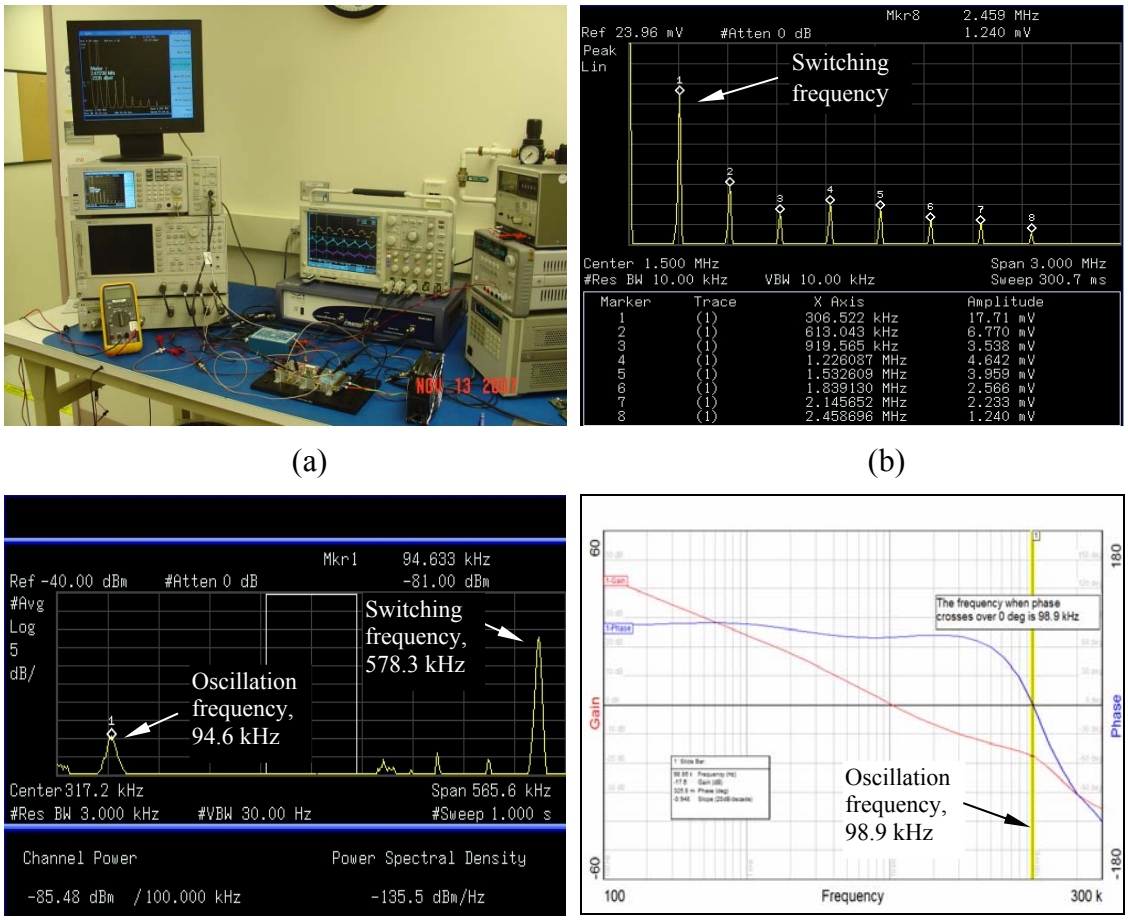

Figure 11: The signal analysis method used to identify the feedback loop oscillation. (a) The signal analysis system, (b) the Fourier spectrum, (c) the power spectrum, and (d) the Bode plot.

The experiments conducted in this study included determining correlations between the oscillation frequencies (in kHz) from a power spectrum (c), and that from readings of a Bode plot (d), as well as correlation relationship between channel power (in dBm) and gain/phase margins (in dB and degree), also in (c) and (d).

3.0 RESULTS AND DISCUSSIONS

3.1 Impedance Measurement for Front-end Oscillation

3.1.1 Varifications of the Input Impedance

It was verified that line voltage change (ΔV_{in}) and load change (ΔI_{out}) resulted in input impedance variations (ΔZ_{in} = $-\Delta R_{in}$) of a DC/DC converter. Figure 12 (a), (b) represent the relationship between input impedance and line voltage and load, respectively. For all models of the DC/DC converters under test, the input impedance ($Z_{in}=-R_{in}=-R_L/D^2$, *and D is the duty cycle*) increased while an input voltage (V_{in}) increased or a load current (I_{out}) decreased, and vice versa. As the result, at full load and low line voltage, the magnitude of Z_{in} was the smallest.

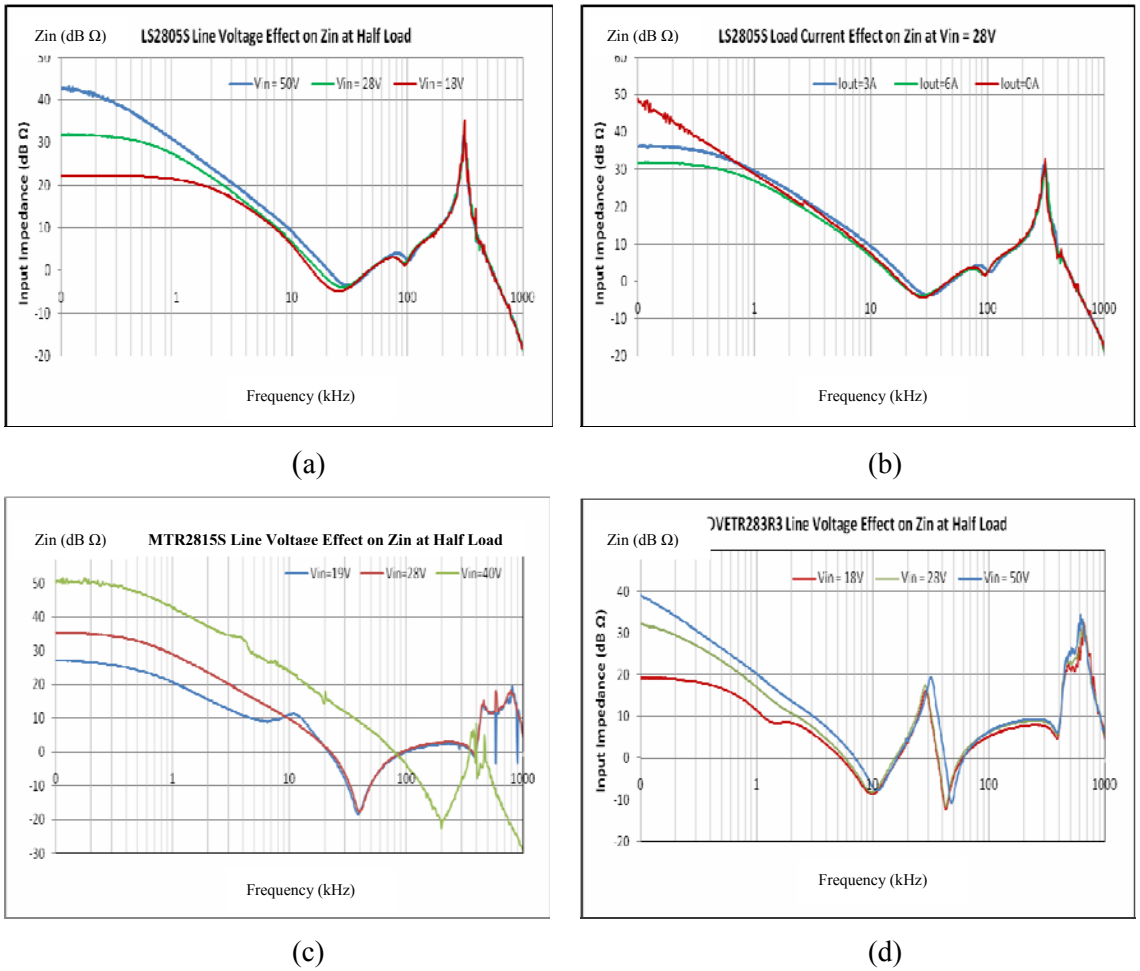

Figure 12: (a) (b) Line voltage and load current effects on input impedance for LS2805S module. (c) Large impedance variation at higher frequency range for MTR2815S. (d) Large impedance variation at low frequencies for DVTR283R3 module.

These characteristics for all modules under test are documented in Appendix B. As shown in all the curves, the input impedance Z_{in} appears as a negative resistance in lower frequency range (0 to 3k Hz, in Figure 12-a, and 0 to 1k Hz in Figure 12-b). In higher frequency range, the input impedance was dominated by control loop bandwidth and power processing elements of the DC/DC converter, and therefore, was no longer appears as a negative resistance. To compare the six modules with input impedance changes at lower frequencies, maximum and minimum magnitudes of the impedance in dBΩ at 100 Hz and 10 kHz were collected at each extreme line and load conditions. The percentage changes of Z_{in} were then calculated and listed in Table 2.

The percent $|\Delta Z_i|$ at the two frequencies for an individual module could indicate how its electrical performance is likely to be degraded by certain external interactions, such as additional input filters. As can be seen, the MTR2815S module has 114.5% of $|\Delta Zi|$ at 10 kHz and 83.5% of $|\Delta Zi|$ at 100 Hz, while the line voltage changed from 19V to 40V. This result may indicate a potential instability risk to this module, because its input impedance varies in large magnitude even at high frequency (up to 200 kHz). The DVETR283R3 module that was in the similar line voltage range also shows a higher $|\Delta Zi|$ of 103% in Table 2, but it was at such a low frequency that the input impedance worked just like a negative input resistance, and possibility of an oscillation could be limited to only at low frequencies.

Table 2: Input Impedance Changes of the Six Converters at Low Frequency (100Hz – 10kHz)

Part No.	Test Condi-tions	At 100 Hz			At 10 kHz		
		$Z_{in,MIN}$ (dB Ω)	$Z_{in,\ MAX}$ (dB Ω)	$\|\Delta Zi\|$ (%)	$Z_{in,MIN}$ (dB Ω)	$Z_{in,\ MAX}$ (dB Ω)	$\|\Delta Zi\|$ (%)
LS2805S	Line	22.30	42.74	91.66	5.86	8.96	52.90
	Load	31.78	48.94	54.00	6.57	7.28	10.81
DVETR283R3	Line	19.32	39.26	103.20	-8.53	-8.04	6.09
	Load	25.57	37.92	48.29	-8.02	-7.44	7.80
DVETR2815D	Line	21.58	38.51	78.45	-8.57	-7.53	13.81
	Load	23.90	37.48	56.82	-8.95	-7.44	20.29
MSA2815D, #1	Line	28.82	49.31	71.10	22.14	25.04	13.09
	Load	29.82	52.20	75.05	22.14	21.32	3.85
MSA2815D, #2	Line	30.93	50.05	61.82	18.48	23.75	28.52
	Load	30.93	51.97	68.02	18.48	20.02	9.31
MTR2815S	Line	27.28	50.05	83.47	11.07	23.75	114.54
	Load	28.22	49.89	76.79	10.03	9.70	3.40

3.1.2 Front-End Oscillation of the Converter

The front-end oscillations were observed several times for every one of the modules under test, when a winding of a signal injection transformer as an extra inductance was inserted into the input power line of those DC/DC converters. Some interesting findings are as follows:

(A) The oscillation appeared to be a sine-wave noise of low frequency, high amplitude on top of the input DC voltage, and it occurred only at input of the converter. The frequencies of the oscillation varied from 600 Hz to near 2 kHz, and the amplitude presented voltages from half volt AC to 85 V_{p-p}, depending on the load conditions and the stages of the oscillation occurrence. Front-end oscillation waveforms of an IR AFL2805S module are shown as Figure 13 (a) (b). Figure 13 (a) was at an early stage of the oscillation, running in 719 Hz and 35.8 mV_{p-p} under 28*Vin* and 1.0A load, while the (b) was at a later stage of the oscillation, running in 725 Hz and 48.4 V_{p-p} under 28*Vin* and 7.0A load. Figure 14 shows the frequency and oscillation amplitude changes versus the load changes for the MFL2812S module. Notice that the maximum amplitude reached to a very harmful level, as high as 85 V_{p-p} at a 5A load. More front-end oscillation images for AFL2805S and MFL2812S are shown in Appendix C.

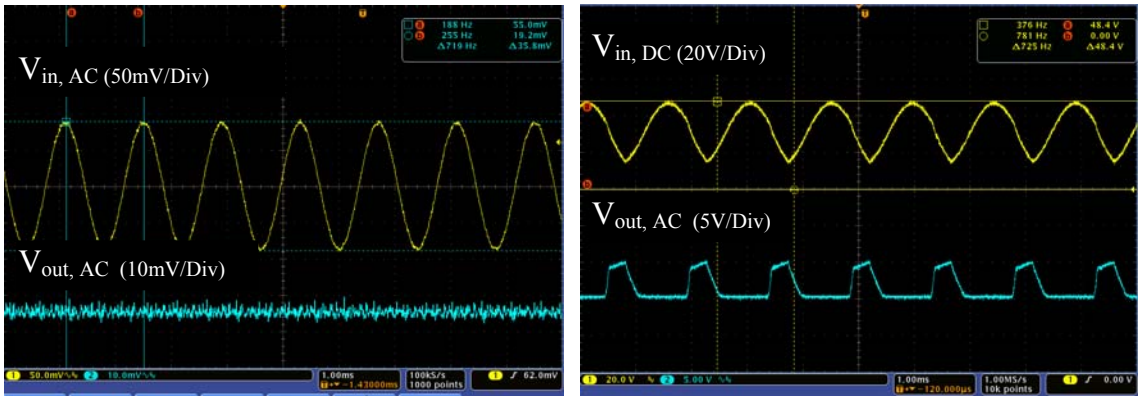

(a) (b)

Figure 13: Front-end oscillation waveform of IR AFL2805S with a filter module. (a) Early stage oscillation waveforms. (b) Later stage waveforms.

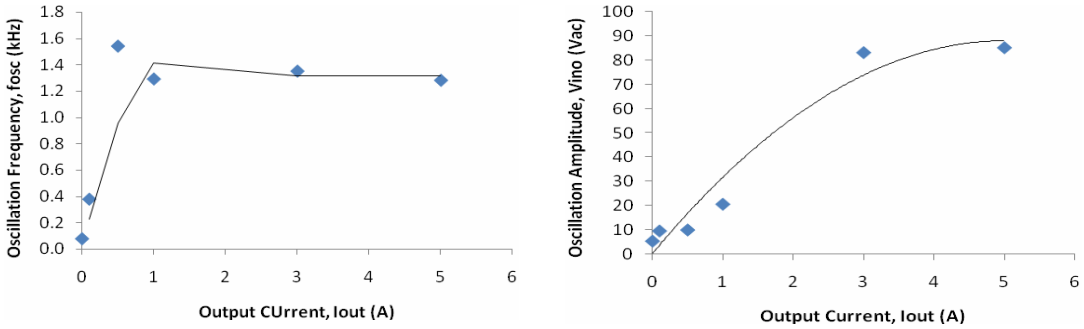

Figure 14: Front-end oscillation frequency and amplitude at different load current for MFL-2812S module at 28VDC input voltage.

(B) The front-end oscillation occurred under certain conditions. It appears that the oscillation was definitely related to the power source output impedance change due to the insertion of a large amount of inductance. The oscillation was also observed to start at certain combinations of input voltages and load currents. Figure 15 shows a curve generated from AFL2805SX test data to demonstrate the occurrences of the oscillation in different power conditions. Notice that an oscillation event occurred only in a correspondent power condition, such as 2A I_{Load} and 22V V_{in}, or 5A I_{Load} and 33V V_{in}. This phenomena implies that the input impedance for this converter no longer meets the input stability requirement ($Z_{source} < Z_{in}$), and it causes the input filters of the converter to oscillate. That input impedance was proven the one derived from the power condition combinations listed in the Figure 15, and it seems to be a single fixed value, no matter which combination it was.

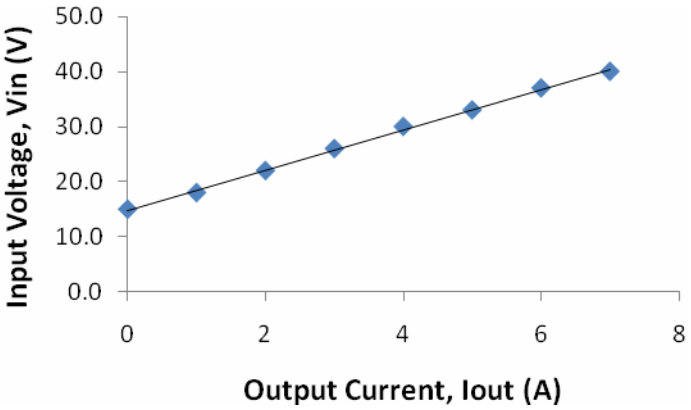

I_{out} (A)	V_{in} (VDC)
0	15
1	18
2	22
3	26
4	30
5	33
6	37
7	40

Figure 15: Front-end oscillation occurrences at different input voltage and output current conditions for the AFL28105SX module.

(C) The oscillation frequencies, noise amplitudes, and power conditions of a starting point were shown to be different for models from different vendors, and to modules with and without an input filter. This information was compared in Table 3. As can be seen among the three nearly identical modules, the input voltages to cause oscillation to start varied from 17.2V to 31.6V, and the oscillation frequencies were doubled when a converter did not have an input filter module connected.

Table 3: Comparisons of Front-End Oscillation for Three Models at I_{out} = 1A.

Models / Parameters	AFL2805S		MFL2812S		DVFL2812S	
	with filter	no filter	with filter	no filter	with filter	no filter
Freq. (kHz)	0.671	1.060	0.730	1.852	0.678	1.400
$V_{in,\ AC}$ (VAC)	1.403	10.82	0.844	3.145	7.211	24.00
$V_{in,\ DC}$ (VDC)	17.20	20.10	22.10	31.90	21.60	31.60
$V_{p,\ ½AC+DC}$ (V)	17.90	25.51	22.52	33.47	25.20	43.60

(D) The front-end oscillation appeared to be independent from feedback loop oscillation. Experiments show that the front-end oscillations did not drive the feedback loops into oscillation even through the oscillation grew up to a high frequency and a high amplitude. This was verified by measuring gain/phase margins while the oscillation was starting. In each case during the testing, the oscillation was allowed to occur only few seconds to get data recorded to avoid a serious damage to the converter.

3.2 Gain/Phase Margin Measurement for Feedback-Loop Oscillation

Gain/phase margin measurement was demonstrated as an accurate and efficient method to determine a feedback loop stability status. However, limitations to access to a noise injection points were the major problem to adopt this method in space flight parts testing. This study explored several options to make this method more practical, and is discussed below.

3.2.1 Measuring Gain/Phase Margin through Remote Sense Terminals

Eight typical hybrid DC/DC converters from three leading space manufactures have shown their abilities to have gain and phase margin measured through remote sense terminals. For those models such as AFL2805S, ATW2805S/EX, MFL2805S, DVTR283R3S, and DVFL2812S, the test probes were directly connected to the correspondent sense pins, and several nice and clean Bode plots showing gain/ phase margin and slope information were obtained. For model MFL2812S, MTR2805SF, and MTR2812S, an external 100Ω resistor was connected between V_{out}+ pin and *Sen*+ Pin, because the internal resistance between these two pins was too high to accurately perform the measurement. Figure 16 (a) and (b) show the photos of the test probe setup and the external resistor connection. The Bode plots of MFL2805S and ATW2805S/ES are shown in Figure 17. While the MFL2805S presented quite normal gain/phase margins, the ATW2805S/ES test module showed a serious problem within the Bode plot. The slope of the gain when passing across 0dB was noticed to be not following the shape of -1 (20dB/decade), so that the gain margins at all load conditions except the light load became small enough to cause an oscillation. The Bode plots for other six test modules are shown in Appendix D.

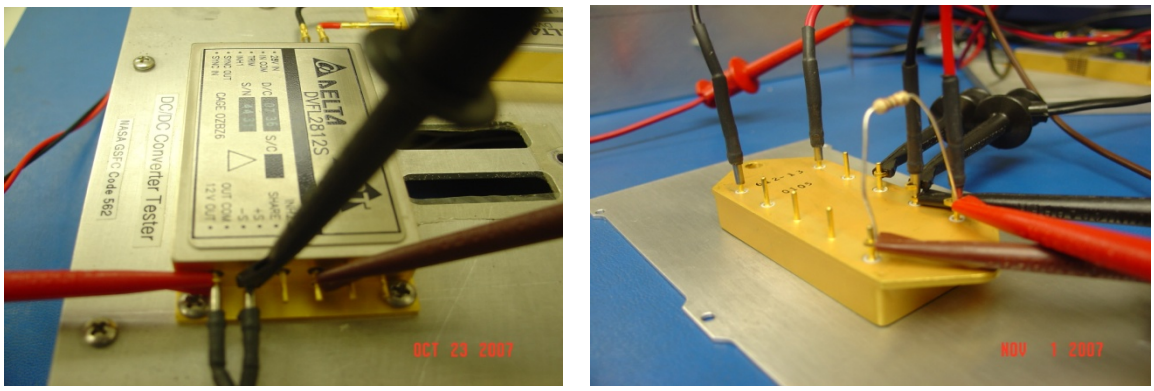

(a) (b)

Figure 16: Gain/phase margin measurement through remote sense pins. (a) Direct connection with test probes. (b) External resistor connection.

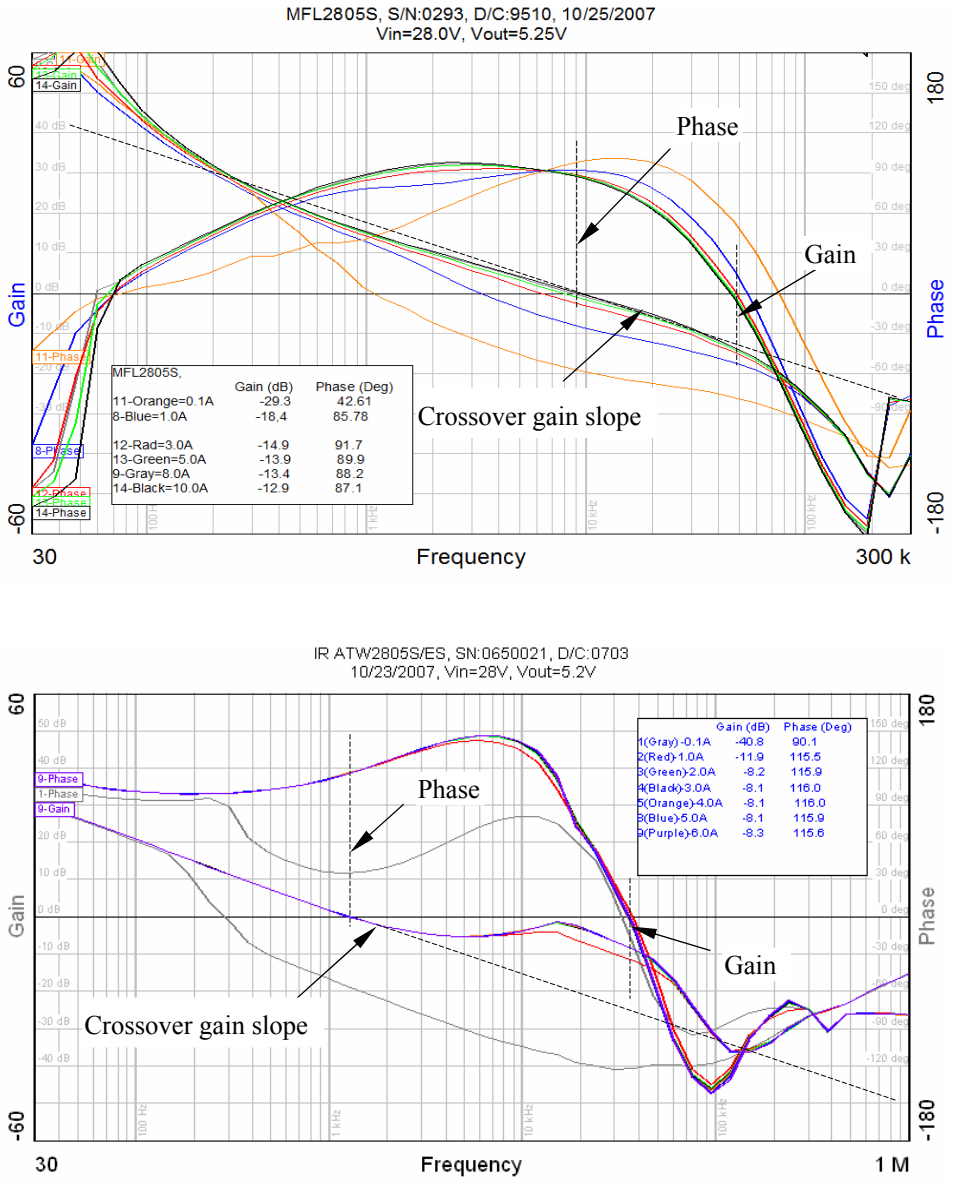

Figure 17: The Bode plots for MFL2805S and ATW2805S/ES showing gain/ phase margins and crossover gain slope.

3.2.2 Measuring Gain/Phase Margin on Open-lid Hybrid Modules

Adopting the open-lid measurement method was attempted on a MFL2812S module, and Bode plots showing gain/phase margins at different power conditions were generated as shown in Figure 18(a). The preliminary result supports the technique of directly probing the resistor inside the module for noise signal injection. Compared to the test result of the external resistor connection (external-R) method shown in Figure 18(b), the open-lid method was able to provide similar measurement in terms of initial gain/phase, slopes of crossover gain and phase, and gain crossover frequency variations due to load condition changes. Figure 19 (a) and (b) illustrates a statistical analysis result on how the two methods are related to each other.

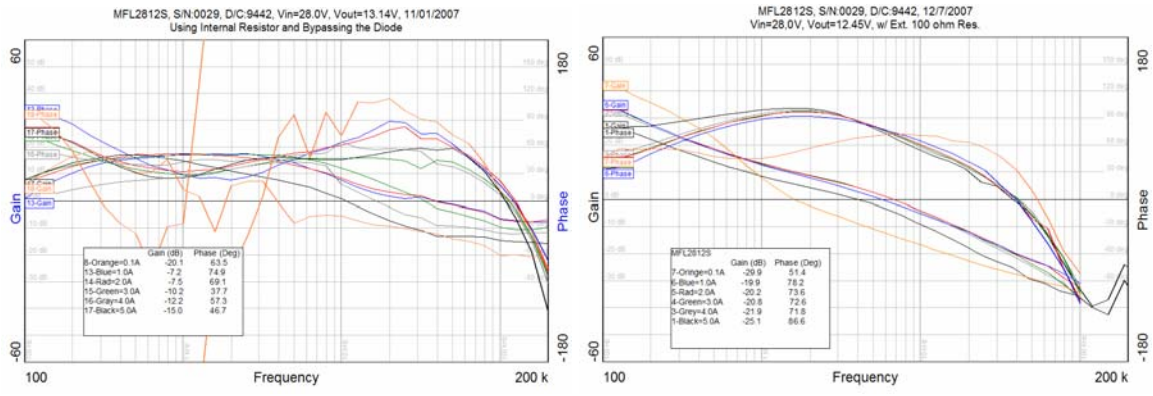

(a) (b)

Figure 18: (a) The Bode plot of MFL2812S using open-lid method, compared to the Bode plot of the same module using external-R method in (b).

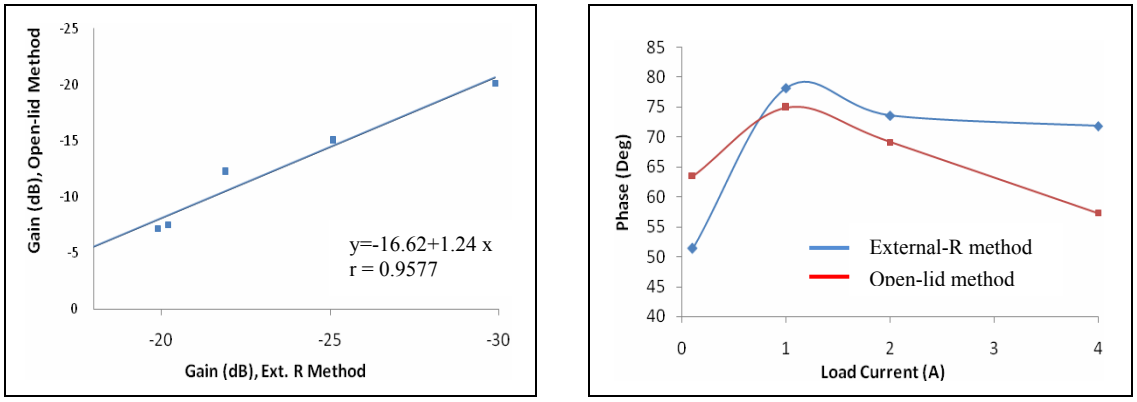

(a) (b)

Figure 19: Measurement method comparisons for open-lid and external-R methods, using data derived from Figure 18. (a) Correlation of the gain between the two methods, and (b) phase change tendencies as the load currents change for the two methods.

With correlation coefficient r = 0.9577, it appears to be strong positive linear relationship between the external-R and open-lid methods for loop gain measurements. The phase measurement data of the two methods does not appear similar, but the tendency to correspond with each other is obvious. It is true that more sample data are needed to get more accurate and better predictions on this relationship.

3.2.3 Electrical and Environmental Effects on Gain/Phase Margins

Gain and phase margins were greatly affected by electrical conditions of converters under the test, and by operating conditions the converters underwent, especially the load current and parts value changes.

The Load Current Effects The load current changes caused gain and phase margin to vary as much as 70%, according to the data from eight DC/DC converters. This was especially true at light load conditions. At higher load to full load, the gain/phase margins kept fairly constant for all modules under the test. Notice that some models always remained in safe gain/phase margins

no matter how much load were varied, while others shifted between safe and unsafe margins when the load changes. That means a DC/DC converter may not oscillate at some load conditions but may start oscillating at another. The test result clearly suggests that checking gain/phase margins at all load levels is critical to ensure the converter's stability. Detailed data on load current effects of the eight converter modules tested are documented in Appendix E.

The Base-plate Temperature Effects When base-plate temperatures of the two AFL2805S and DVFL2812S modules were varied from -55°C to 125°C, the significant changes of gain and phase margins were observed from all test settings. Table 3 shows some larger values of gain/phase margin percent change obtained from the temperature test, and the complete data is listed in Appendix (F) and (G). The Δ Margin %, a percent change of a margin, was defined as percentage changes of gain or phase values when the temperature changes from -55°C to 125°C. As can be seen among those data, the largest percent changes of gain and phase were 24.5% and 19.8 % for AFL2805S, and 37.6% and 31.9% for DVFL2812S, respectively.

Table 3: Gain/ Phase Margin Percent Changes Affected by Base-plate Temperature at Several Power Settings (ΔT: -55°C ~125°C).

	AFL2805S		**DVFL2812S**	
	V_{in} (V)/I_{out} (A)	Δ Margin (%)	V_{in} (V)/I_{out} (A)	Δ Margin (%)
Gain margin	16 / 5	19.3	40 / 1.0	37.6
	28 / 10	24.5	28 / 3.0	32.8
	28 / 15	12.0	16 / 6.0	11.2
Phase margin	28 / 5	9.7	40 / 1.0	31.3
	28 / 10	13.9	40 / 3.0	29.3
	16 / 16	19.8	16 / 6.0	31.9

The two modules were also tested for their switching frequency stabilities during the test when the temperature was varied from -55°C to 125°C. Phenomena of switching frequency instability were observed when monitoring the switching waveform power spectrum at vendor specified frequency. As the temperature went up, the frequencies of maximum center power amplitudes moved down. Those tendencies can be clearly seen in Figure 20 (a) and (b) for the two modules. In fact, the switching frequency of DVFL2812S dropped 14.9% from the nominal 550 kHz at 40°C to 468 kHz at 126°C, while the AFL2805S module presented only 2% drift from nominal 575 kHz down to 562 kHz within the similar temperature range.

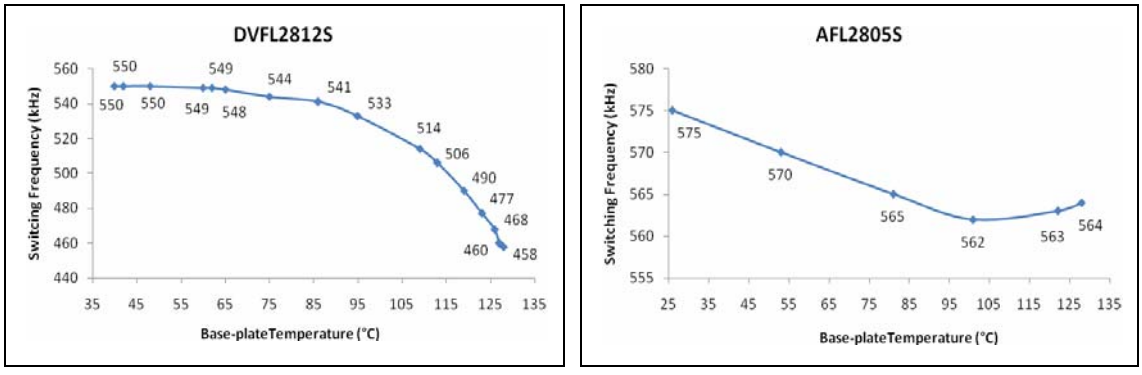

(a) (b)

Figure 20: Switching frequency drifts affected by base-plate temperature variations for the two modules.

The Feedback Loop Compensation Network Components Value Effect Component values change of a feedback loop compensation network demonstrated effects on gain and phase margins, gain slope, and gain and phase crossover frequencies. The open-frame DC/DC converter module, QV24-5-25, were tested for the comprehensive effects, where the compensation network resistors R6 and capacitor C6 were changed in their values. This test used C_v6 with a fixed value of 560 pF and R_v6 with an adjusted value from 1kΩ to 10kΩ. The tendencies of the effects are shown in Figure 21 below, and the Bode plot and the measured data are provided in Appendix H.

The original design of this converter assigned the R6 and C6 with nominal values of 10kΩ and 3900pF to permit a stable operation with -10.4 dB and 72 degree gain/phase margins and a -1

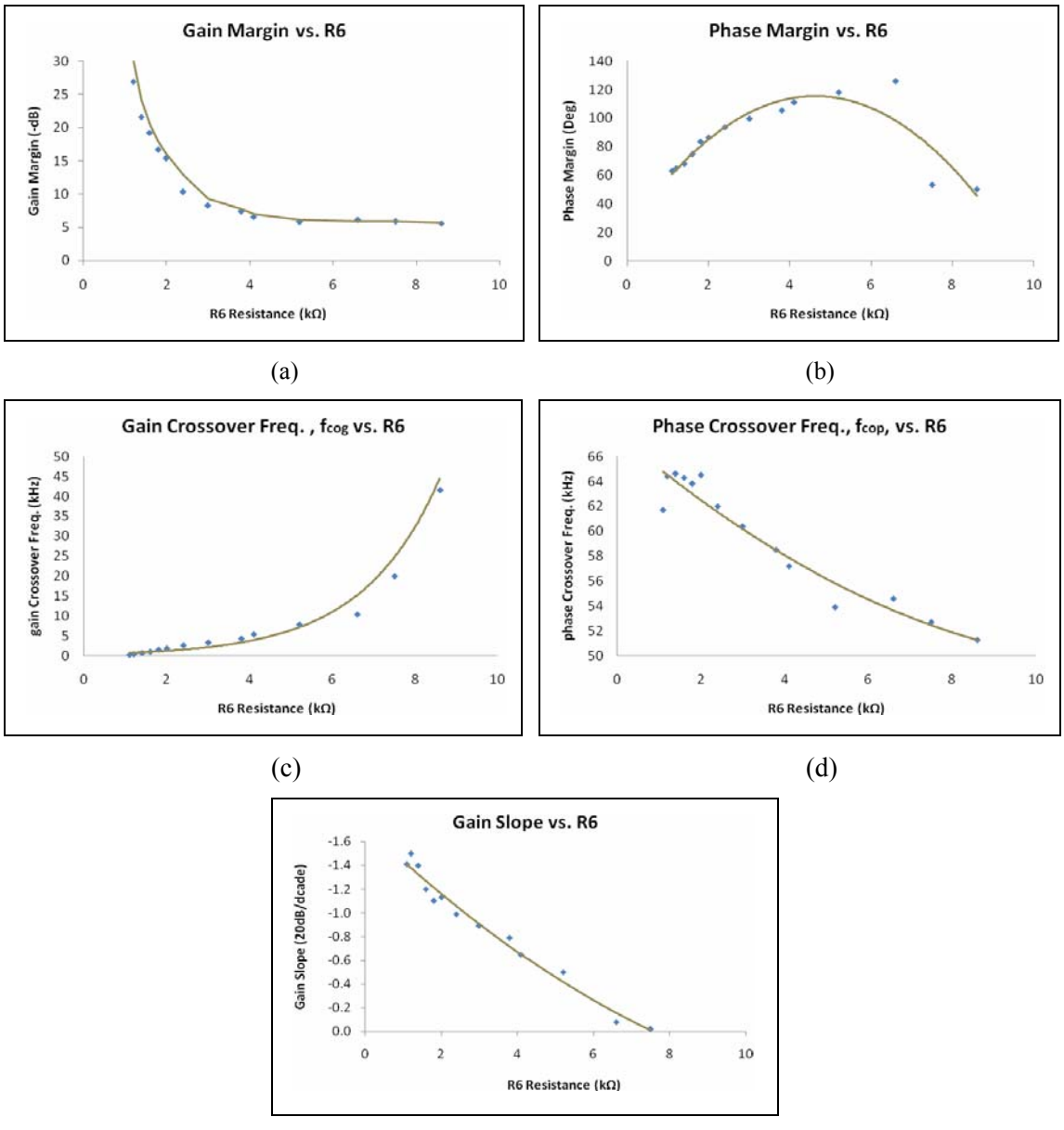

Figure 21: The component value change effects of compensation network R6 on five feedback loop performance parameters.

slope at 28V input and 5A output power conditions. When C6, during the test, was reduced from 3900pF to 560pF, the converter immediately stated oscillating. In order to restore the converter stability, the resistor R6 was reduced from 10kΩ to about 2kΩ to obtain the gain/phase margins and the slope to around -10dB, 70 degree, and -1 slope, respectively, and it was shown in Figure 21 (a), (b) and (e). The curves show that the gain margin was reduced 78.8% when R6 value was increased from 2kΩ to 10kΩ and the phase margin moved up almost linearly to its highest point of 125.7 degree, a 50% increase from the margin at 2kΩ. After increasing the R6 to 6.6kΩ, the converter appeared to go unstable and eventually started oscillation, because of the low gain margins and the very low gain slopes. Notice that the gain crossover freqency was shifted down to very low range at about 300 Hz, eventhough the converter appeared stable. Indeed, the potential instability was obvious because it showed a design rule violation, which requires the crossover frequency to be at least one-fifth the switching frequency, or 60 kHz in this case. Also notice that althogh the phase crossover frequency drifted 20% when R6 was varied from 2kΩ to 10kΩ, the phase margins within these frequencies were still large enough for the converter's stable operation.

3.3 Oscillation Identification and Early Detection Using Spectral Analysis

The new approach to detect feedback loop oscillation based on spectral analysis of the input voltage noise showed a great advantage over the gain/phase margin measurement using frequency response analysis, especially for those hybrid DC/DC converters without remote sense terminals. A practical feedback-loop instability indicator utilizing combined information of channel power magnitude and a specified frequency provided an effective technique to identify the oscillations at early stages. The effectiveness was evaluated by distinguishing the oscillation frequency from other frequencies and by comparing the channel power magnitude with the corresponding gain/phase margins derived from the Bode plot.

3.3.1 Feedback Loop Oscillation Frequencies

As discussed early, one of the requirements for a DC/DC converter to be stable is that the feedback control loop gain must be less than unity (< 0 dB) when the loop phase is a total of 360°. This criterion implies that in case the gain reaches 0 dB and an interacted noise has a frequency (including the harmonics) that is the same frequency when the phase crosses over the unity gain of 0 dB so that the noise signal at input and output of the feedback loop becomes in phase, an oscillation must be ringing at the phase crossover frequency. Based on this concept, there must be a significant noise amplitude in an input voltage noise spectrum at the phase crossover frequency.

The oscillation simulator used in previous test was used here again to create an adequate oscillation so that the oscillation noise signal was captured in a power spectrum. One of the power spectrum images is shown as Figure 11(c) in page 10. In order to prove the existence of the oscillation frequency, a corresponding Bode plot in Figure 11(d) was taken at the same condition as the power spectrum was obtained. As can be seen, the crossover frequency of 98.9 kHz measured in the Bode plot, was detected in the power spectrum as 94.6 kHz with only 4.5% difference. To further investigate the correlation between the two frequencies in QV24-5-25, 18 phase-crossover frequencies and 18 correspondent channel power frequencies were measured simultaneously while adjusting the simulator to generate 18 incremental noise levels. The test result showed that the two frequencies had strong relationship with a correlation coefficient of r = 0.9453, and 89.4% of the variability in power spectrum readings were accounted by the Bode plot readings. Figure 22 (a) (b) represents the correlation between the two frequencies for the QV24-5-25 converter.

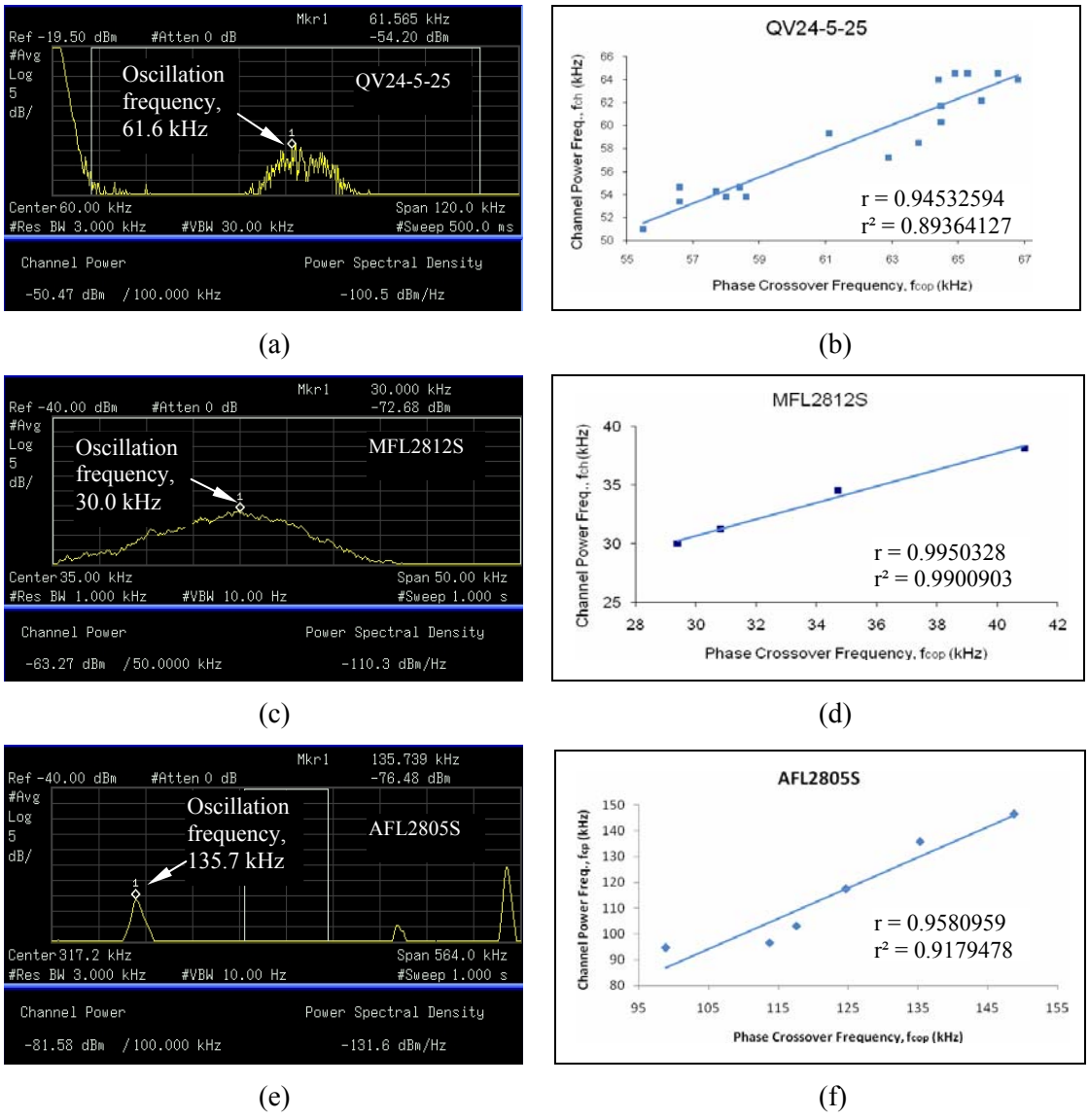

Figure 22: Power spectra showing oscillation frequencies (left), and correlation between oscillation frequency and phase crossover frequency for QV24-5-25, MFL2812S, and AFL2805S modules (right).

Testing on hybrid converters such as MFL2812S and AFL2805S to evaluate the relationship between the two frequencies presented very similar results as the QV24-5-25. As can be seen in Figure 22 (c) to (f), there was obvious pulse amplitude at the phase crossover frequency of each module, and each of the frequency change truly caused a corresponding change of a frequency measured from the power spectrum. The correlations were very strong for the two trend lines with values r = 0.9950 and r = 0.9581, respectively. Notice that the three power spectra look very different from each other because the measurement settings of the spectrum analyzer, such as resolution bandwidth, center frequency, span, and reference, were set differently in order to get relatively good readings.

In general, the feedback loop oscillation frequency was determined to be in a high frequency range, was unique for every individual type of the converters, and showed strong linear

correlation with the phase crossover frequencies presented in Bode plot of the gain/phase margin measurement. The raw data for those measurements is listed in Appendix I.

3.3.2 New Instability Indicator Approach

The testing showed that the channel power magnitude measured from input noise power spectrum of a DC/DC converter could be a precise indicator for feedback loop instability. Indeed, the channel power magnitude (in dBm) contained total average of oscillation noise energy within a specified frequency range. The average amount of the energy made the channel power reading more stable and more sensitive to the detected signal than the pulse amplitude in a Fourier spectrum as observed in this experiment. It was believed that the channel power magnitude could truly respond to a very small change of oscillation noise merged in the input voltage noise.

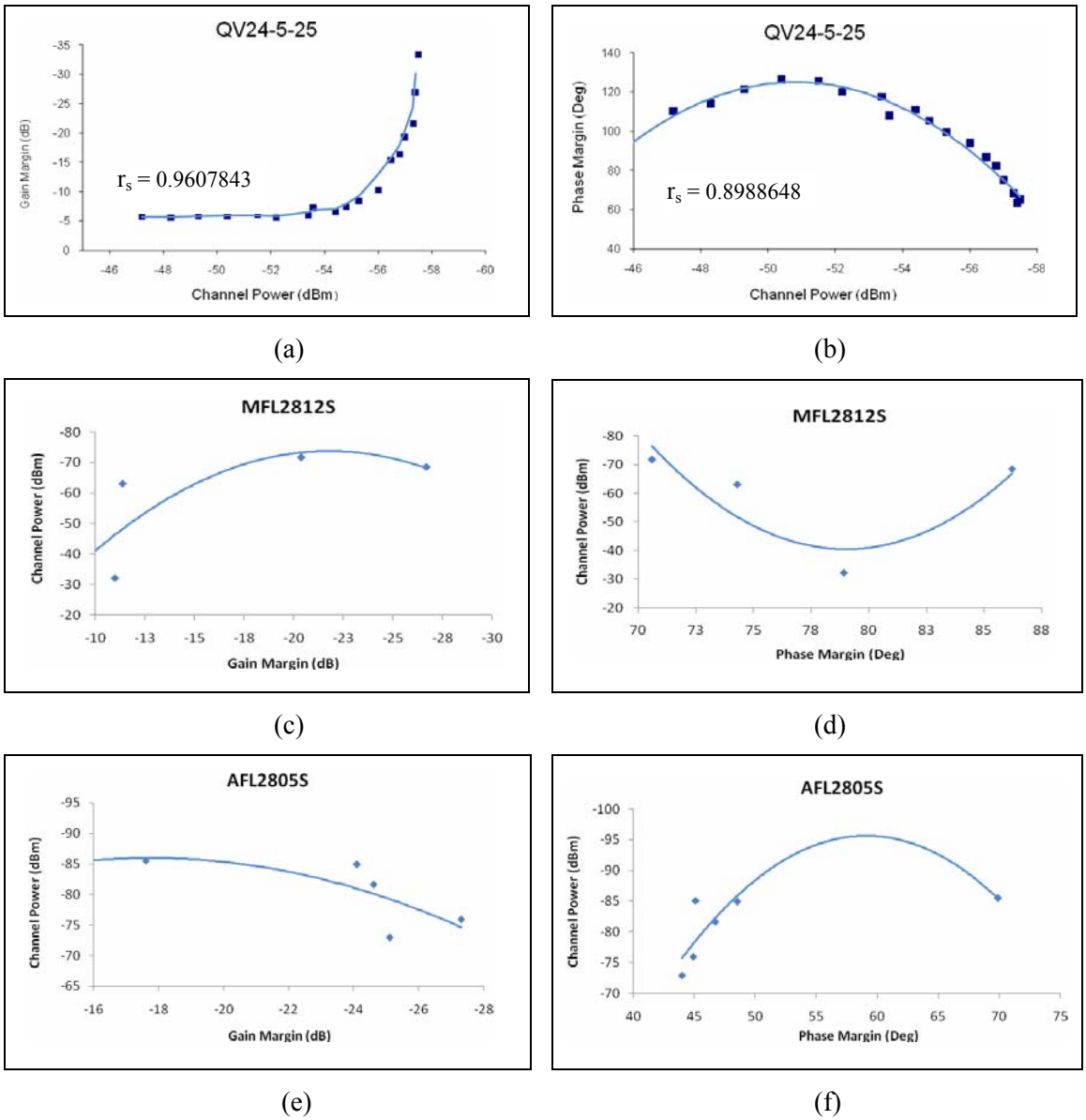

Figure 23: Correlation between channel power and gain and phase margins for the QV24-5-25, MFL2812S, and AFL2805S modules, referring data listed in Appendix I.

The first effort was made to determine if channel power magnitude in the input noise power spectrum had strong correlation with the gain/phase margins measured under the same test condition. Figure 23 (a), (b) shows the relationship between channel power and gain and phase margins, which were obtained using the oscillation simulator containing a QV24-5-25 module. Because the correlation appeared non-linear, a rank order correlation coefficient (r_s) was used to measure whether the channel power (dBm) increased (or decreased) with the gain and phase margins. The data curves indicated a trend that when the channel power magnitude decreased the gain and phase margins increased (or decreased) accordingly, with quite large r_s values equal to 0.9608 for gain margin and 0.8989 for phase margin, respectively. In fact, the lower r_s value simply means that there was a larger portion of negative relationship between the two parameters, compared to the positive relationship showed in Figure 23(b). The two hybrid DC/DC converter, MFL2812S and AFL2805S, presented very similar results as shown in Figure 23(c) to (f). It is true that the curves could give better presentations if more measurement points were contained. With the fewer test data point, however, however, it was already significant for the channel power magnitude and the gain/phase margins to represent each other.

3.3.3 Effectiveness of the Oscillation Indicator

Because of the strong correlation that the channel power showed with the gain/phase margins, it potentially provided a strong capability to detect an input voltage noise generated by feedback loop oscillation. An effort was made to prove that the oscillation indicator is an effective tool to detect the oscillation noise. It was found that the detected oscillation noise at the phase-crossover frequency appeared to have a very small amount of channel power at its initial stage. It developed gradually, as observed on an oscilloscope as a jitter, and continuously grew until it reached full oscillation stage. This process is illustrated in Figure 25.

It was noticed that the detected noise at its early oscillation stage was so small that even the oscilloscope was not able to capture it, as can be seen in the image of Figure 25(a) row right side. The waveform in the middle is the converter input line noise voltage in AC mV, and it has a different frequency as the channel power peak. As a comparison, gain and phase margins were also measured at each of the five oscillation stages, and the Bode plot containing the gain/phase data is shown in Appendix A (b). In the initial oscillation stage, the gain and phase margins were measured to be in a good condition as -23.7 dB and 63.7°. However, the channel power of the noise power spectrum had already indicated an obvious -55.5 dBm noise level. When the noise became a higher level jitter, the gain/phase margin measurement still showed -6.4 dB and 114.8° margins as to be acceptable in most cases.

The power spectra in Appendix J illustrate the similar oscillation noise development stages detected by using the oscillation indicator. The MFL2812S hybrid DC/DC converter that generated this noise appeared to be quite stable at early stages, and there were no jitter signature visible from the oscilloscope. However, the noise was detected by the oscillation indicator when input line voltage and load current were set in somewhat points. It was determined as an early oscillation noise because its frequency between 30 kHz to 38 kHz was the same as the phase crossover frequency measured as 33 kHz to 37 kHz in a previous test. Eventually, as the power condition was set to 20.9V input and 3A output, the converter oscillated badly and a harsh sound was clearly heard.

It should be mentioned that due to the limitation of availiable flight DC/DC converter modules, the study on effectiveness of the oscillation identification and early detection technique was not widely extended to more test smples. However, the priliminary tests provided an interesting and significant experience for further explortion of this test method.

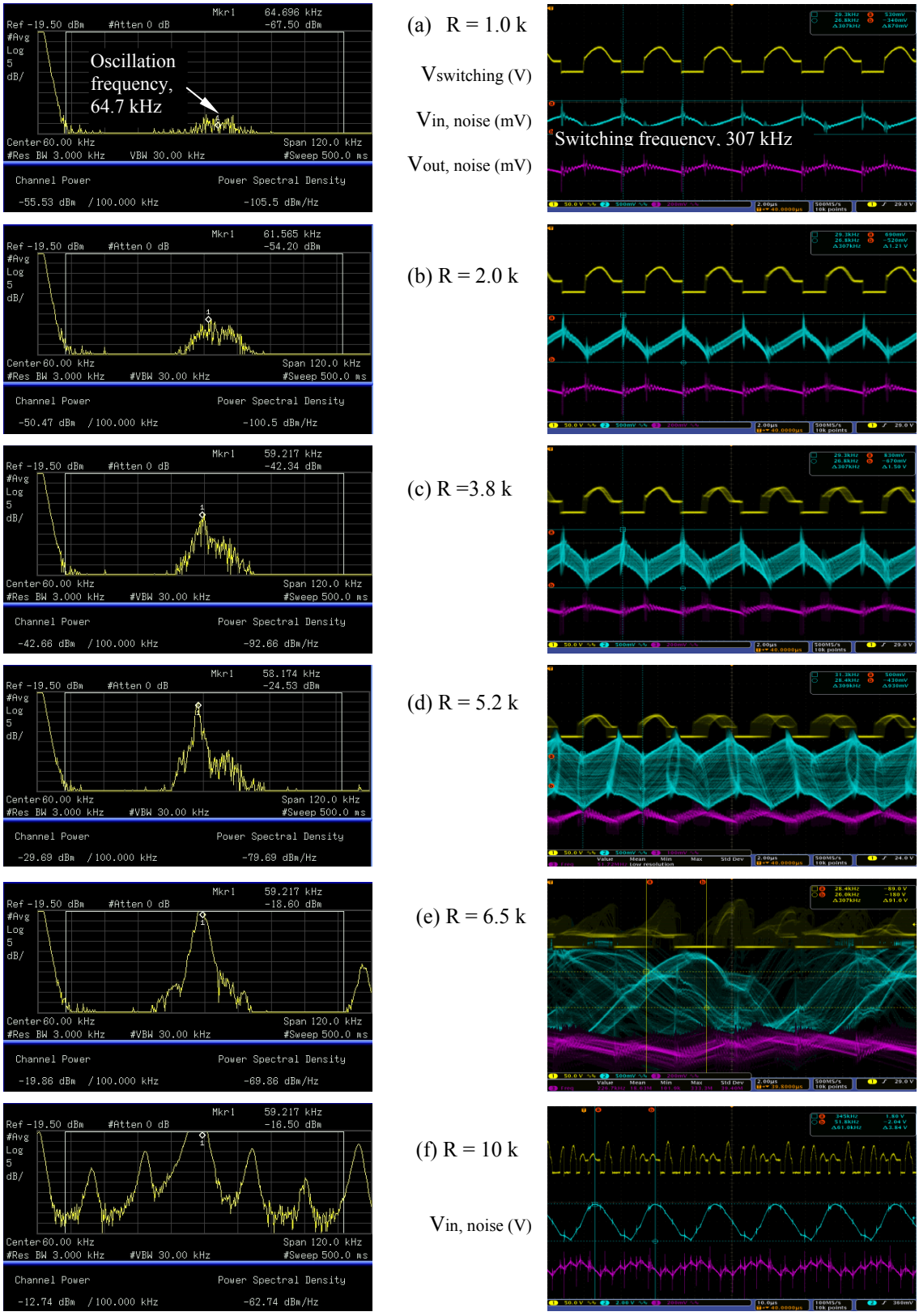

Figure 25: Oscillation development of QV24-5-25 as compensation resistor changes. The images show input noise power spectra (left) and jitters (right).

4.0 CONCLUSIONS

Based on this study, the following major conclusions are drawn:

1. Potential instability problems could exist in flight hybrid DC/DC converters due to the lack of adequate testing for gain/phase margins and the input impedance characterization of the parts by the manufacturer or as part of incoming acceptance test.

2. Possible damages may be caused to the converters due to the lack of proper monitoring and ability to assure the converter stabilities during all phases of flight applications.

3. Temperature and component value changes of the feedback loop compensation network made major contributions to the gain/phase margin variations and the switching frequency drifts.

4. DC/DC converter oscillations could be categorized into front-end oscillation and feedback-loop oscillation, and those two types of oscillations were independent from each other. The front-end oscillation shows up as a low voltage (few volts up to 100V) sine-wave at low frequency (< few kHz) caused by input impedance mismatched with source output impedance, and it could slowly destroy the module. The feedback-loop oscillation was caused by gain/phase related problems. It is presented initially as a low voltage (in mV), high frequency noise (up to few hundred kHz), and may develop into a high voltage (few hundred volts) instantly.

5. It was verified that the line voltage change (ΔV_{in}) and load change (ΔI_{out}) resulted in input impedance variations ($\Delta Z_{in} = -\Delta R_{in}$) of a hybrid DC/DC converter. The input impedance Z_{in} appeared as a negative resistance only in lower frequency range. In higher frequency range, the impedance varied with the frequency and was no longer affected significantly by line voltage and load conditions. The impedance that was affected by the line and load at a higher frequency range may indicate a potential instability problem.

6. Gain/phase margin measurement was demonstrated to be an efficient method to determine the feedback loop stability status for most NASA used hybrid DC/DC converters available with remote sense terminals. This method could be further extended for use in the open-lid units with the similar measurement accuracy.

7. The new approach to detect feedback loop oscillation based on spectral analysis of the input voltage noise showed a great advantage over the gain/phase margin measurement method, especially for those hybrid DC/DC converters without remote sense terminals. It was shown capable in detecting a small level feedback loop oscillation noise that could not be captured by an oscilloscope or determined by the gain/phase margins of Body plot.

8. A Feedback-Loop Instability Indicator was established by adopting a Channel Power magnitude in dBm from a power spectrum of a converter input voltage noise, at a frequency that was proved equal to the phase-crossover frequency existing in the Bode plot. This frequency was unique for every type of the converters, and was sensitive enough to indicate existence of feedback loop oscillation.

9. The gain/phase margin method and the oscillation indicator were well correlated in term of determining stability levels, but they did not linearly represent each other that well

because of their different basic characteristics. However, it was found that the oscillation indicator could detect an oscillation noise even though the gain/phase margin was still shown to be within an acceptable level.

5.0 RECOMMENDATIONS

Based on the test results, the following recommendations are made:

1. Additional development of the oscillation detection technology to make the Feedback-Loop Oscillation Indicator more sensitive and reliable for the oscillation noise signal detection.

2. Expand application of the oscillation detection technology to wider range of hybrid DC/DC converters that are not supplied with voltage sense feature.

3. Perform study on the accuracy of the gain/phase measurement method to identify major possible test errors, which may cause inaccurate or misleading test results. This will include evaluation of the frequency response analyzer, design of flight DC/DC converter test connectivity, and creating related test procedures.

4. Update the MIL standard and NASA power system design and test guidelines to require the testing and monitoring of DC/DC converter stability at part, board, and subsystem test levels.

5. Establish requirement for the manufacturers to provide gain/phase margins, converter input and input filter output impedance measurement data in their datasheets integrated to the basic electrical performance characteristics information.

6. Test all flight DC/DC converters for stability before delivering to flight mission end-users, and provide them with application data and guidelines.

REFERENCES

1. P. K. Harris, and N. F. Block, "Potential Damage to Flight Hardware from MIL-STD-462 CS02 Setup", *IEEE 0-7803-7835-0/03, 2003, pp. 603-606*

2. A. Whittlesey, and K. Erickson, "A Stable CS01 Tester for Switch Mode Power Supplies", *www.albert.whittlesey@jpl.nasa.gov, NASA Contract NAS5-32537,*

3. H. Shaw, J. Shue, D. Liu, B. L. Wang, and J. Plante, "Advanced DC/DC converter Towards High Volumetric Efficiencies for Space Applications", *NASA/GSFC DDF Report, 2005.*

4. SynQor, "Input System Instability, *Application Note" PQ-00-05-1, Rev 01, 2000.*

5. D. H. Venable, "Testing Power Sources for Stability", *Production Applications, Technical Paper#1, www.vanableindustries.com, 2000.*

6. D. H. Venable, "Source Load Interactions in Multi-Unit Power Systems", *AIAA-94-4235-CP, Venable Industries, Inc, 1994*

7. R. Ridley, "Loop Gain Measurement", *Switching Power Magazine, 2005, pp. 1-3*

APPENDICES

Appendix A: (a) The schematic of feedback loop oscillation simulator, and (b) Bode plot for oscillation noise detection by changing R6 resistance of the feedback loop network..

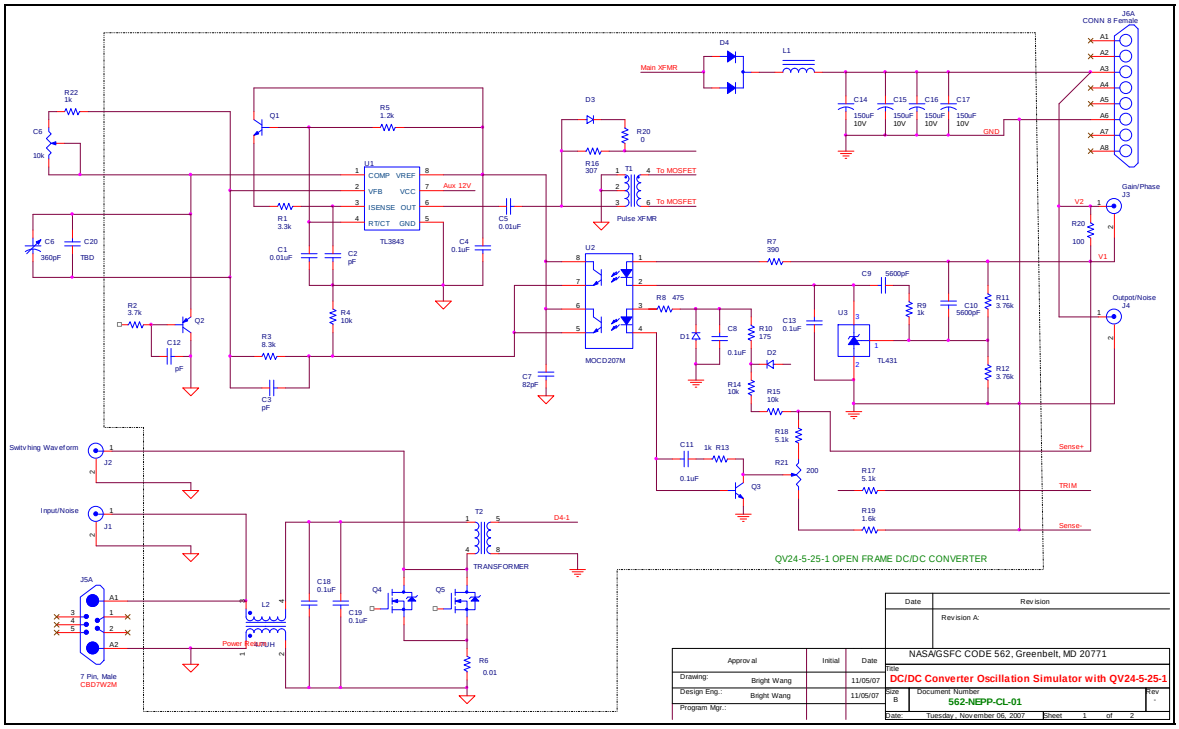

(a)

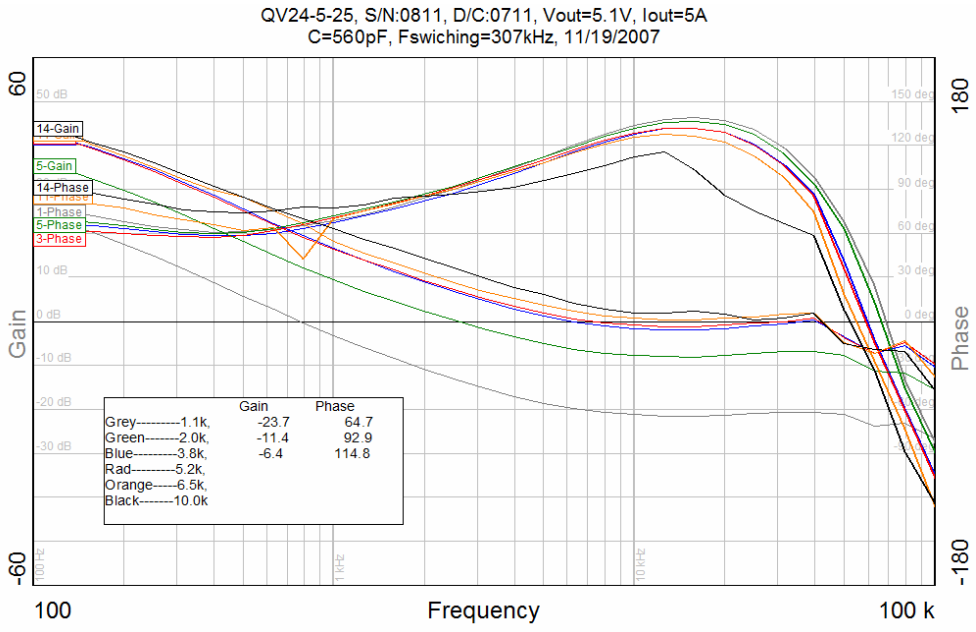

(b)

Appendix B (1): Line voltage and load effects on input impedance for three different DC/DC converter models, (a) (b) IR LS2805S; (c) (d) VPT VETR28R3; and (e) (f) VPT DVETR2815D.

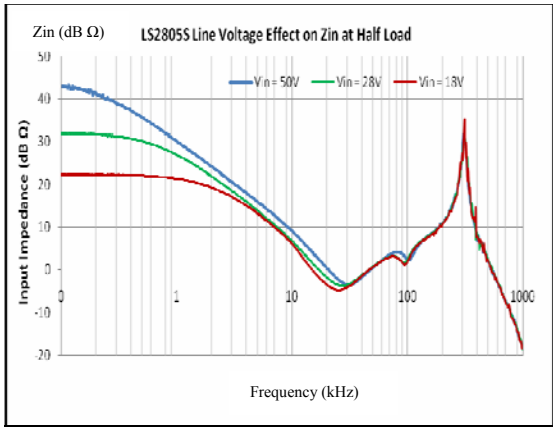

(a)

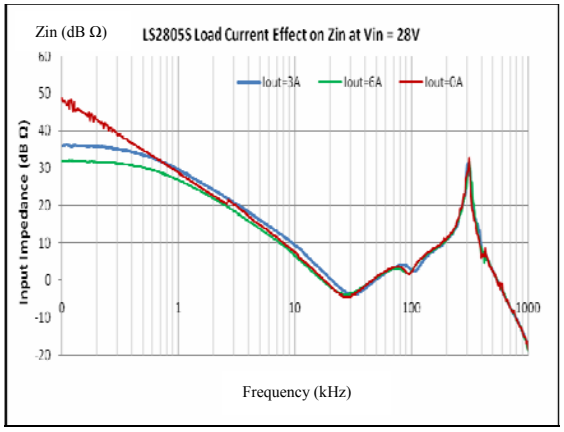

(b)

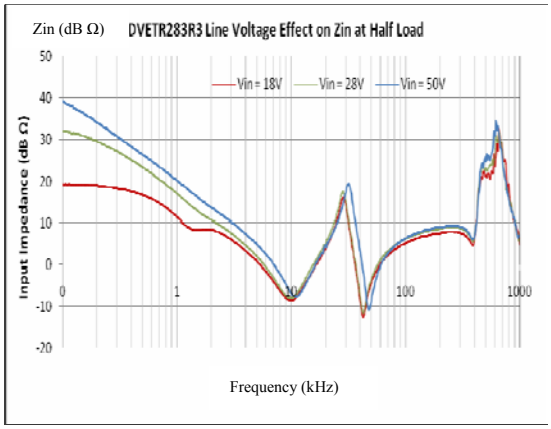

(c)

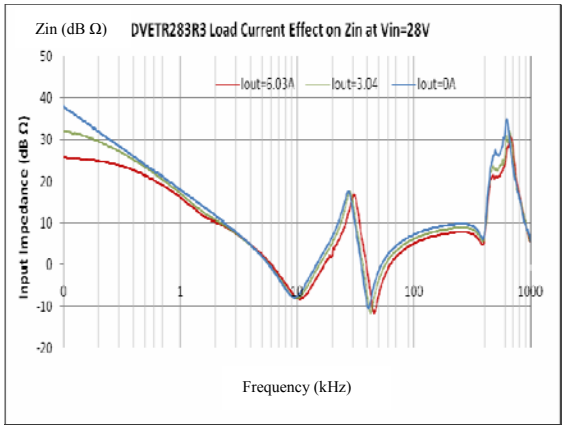

(d)

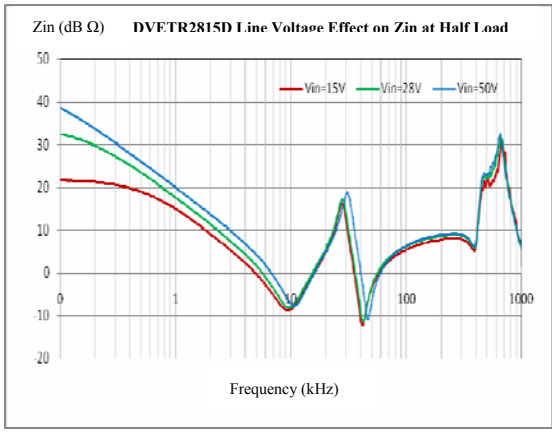

(e)

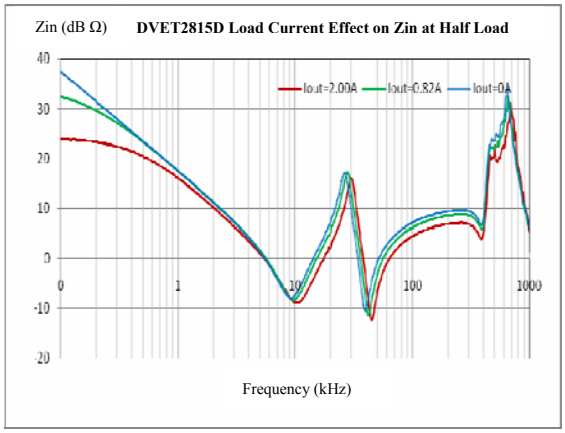

(f)

Appendix B (2): Line voltage and load effects on input impedance for three different DC/DC converter models, (a)(b) Interpoint MSA2815D, #1; (c)(d) Interpoint MSA2815D, #2; and (e)(f) Interpoint MTR2815S.

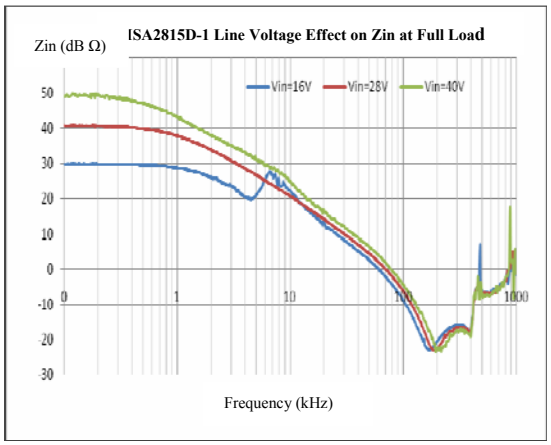

(a)

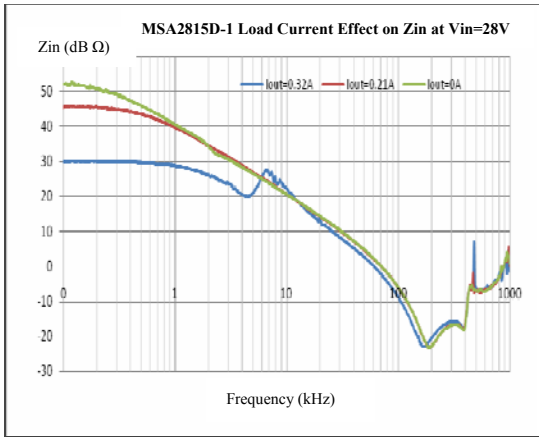

(b)

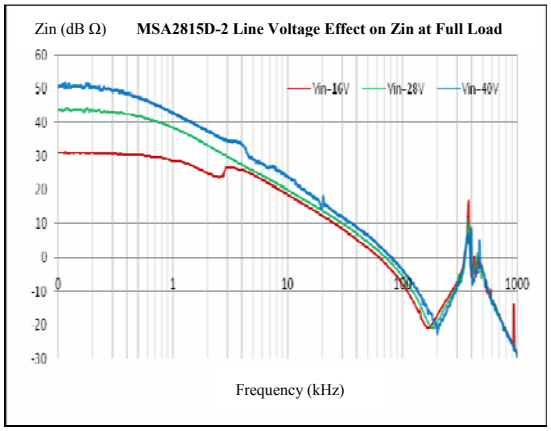

(c)

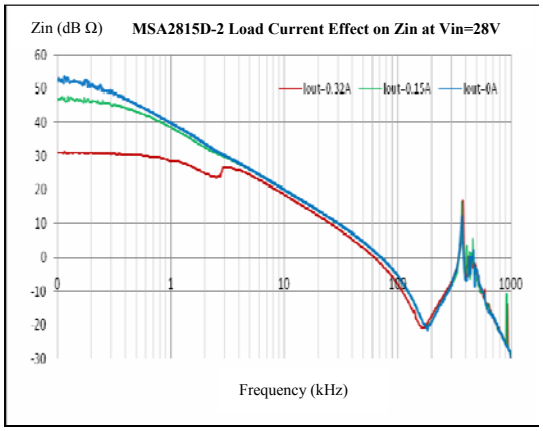

(d)

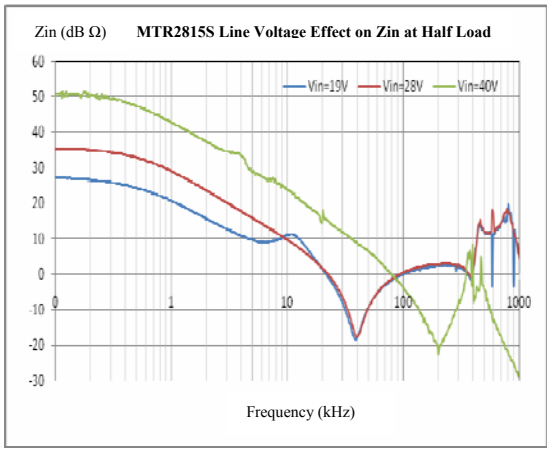

(e)

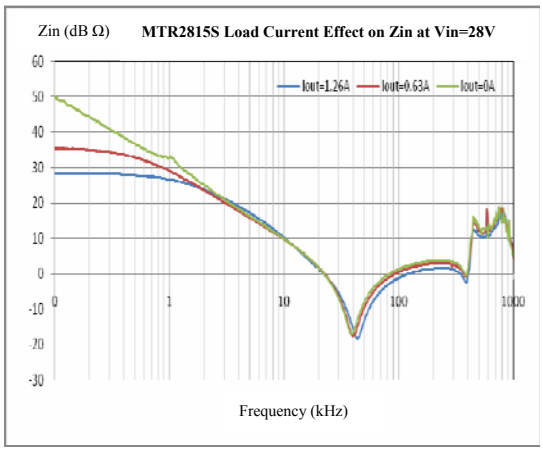

(f)

Appendix C: The frond-end oscillation development waveforms of AFL2805S with an input filter, AME2828461X/ES. Waveform (a) and (b) was at early oscillation stage with load current 1A and 5A, respectively. Figure (c), (d) and (e) shows waveforms at later stage of the oscillation with load current of 1A, 5A, and 7A, respectively. Figure (f) shows a MFL2812S at early oscillation stage with 1A load, running at 1.72 kHz. Upper trace: V_{in} noise in Volt, Lower trace: V_{out} ripple in mV.

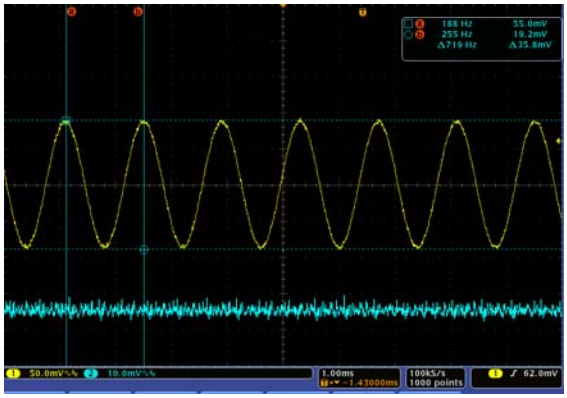

(a)

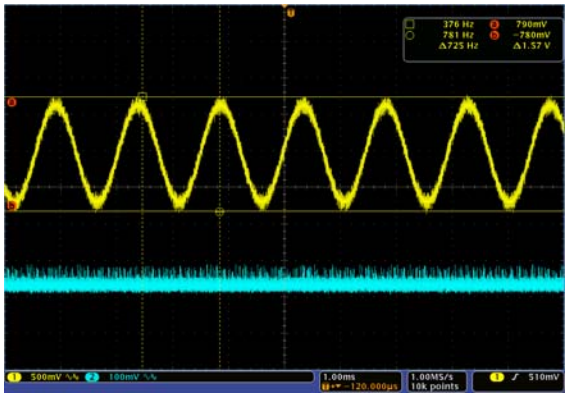

(b)

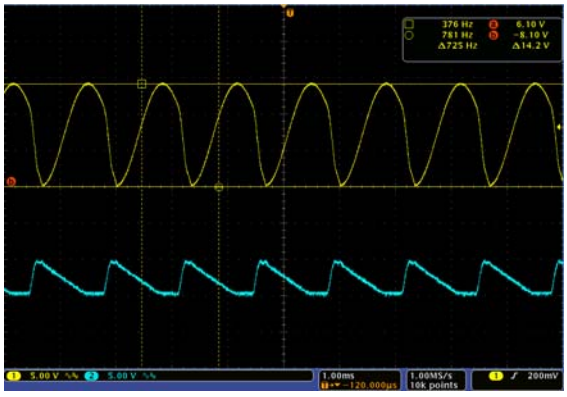

(c)

(d)

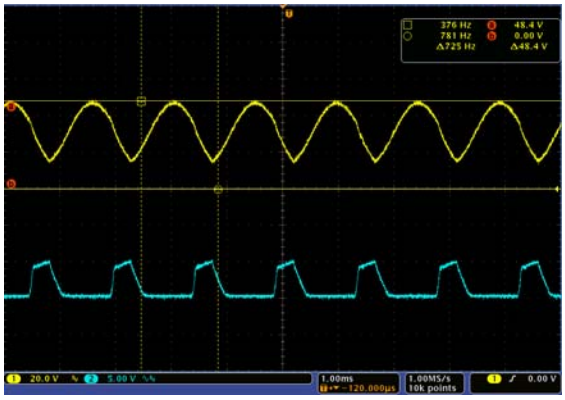

(e)

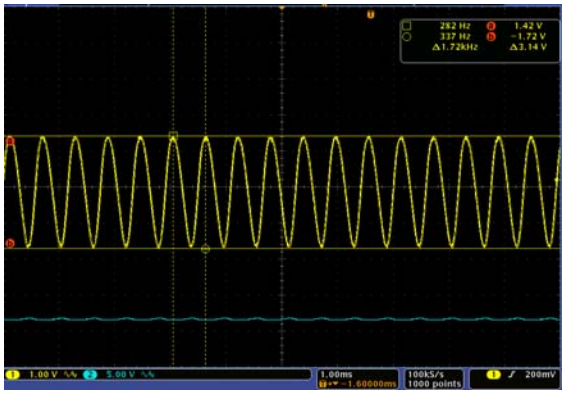

(f)

Appendix D: Figure (a) to (f) shows Bode plots for six of the eight modules under Test.

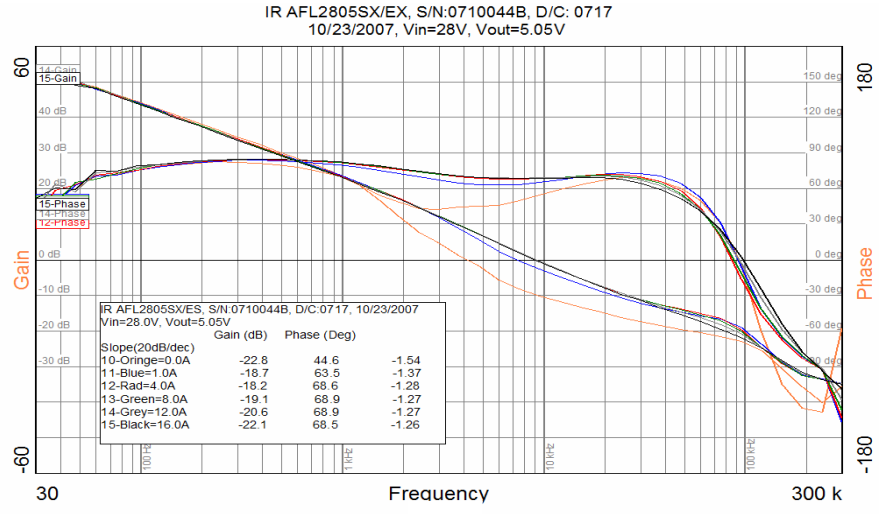

(a)

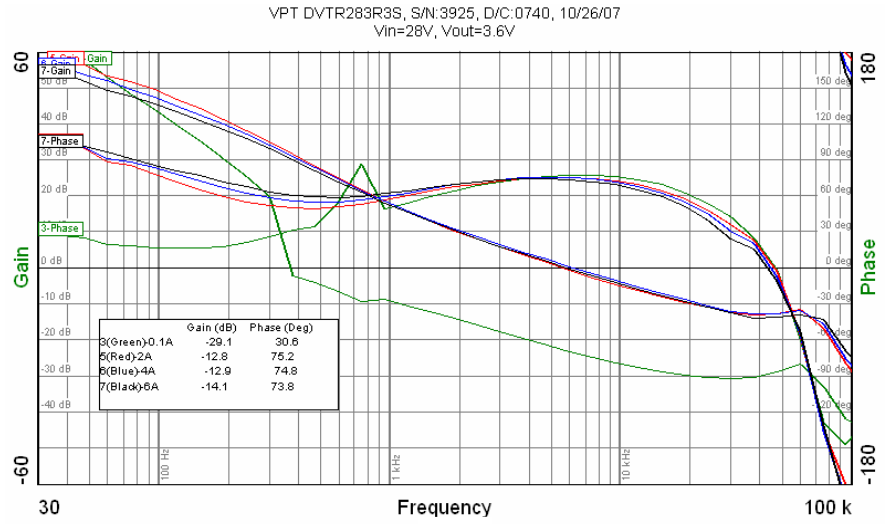

(b)

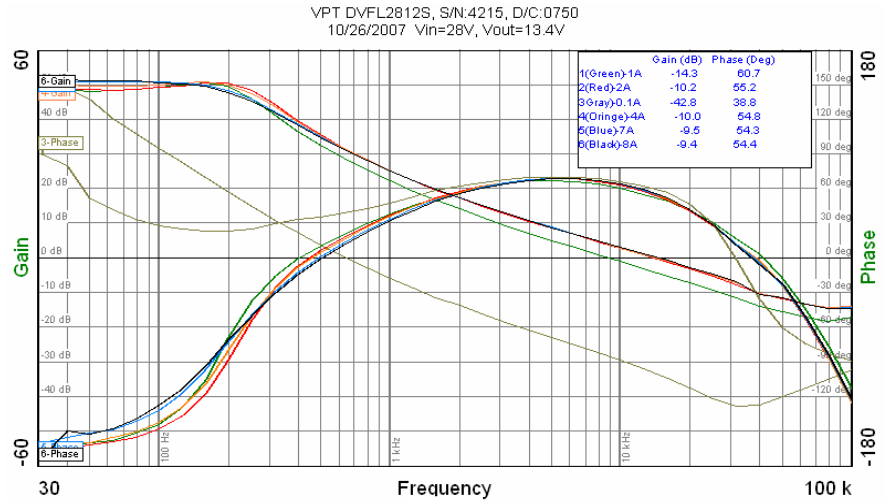

(c)

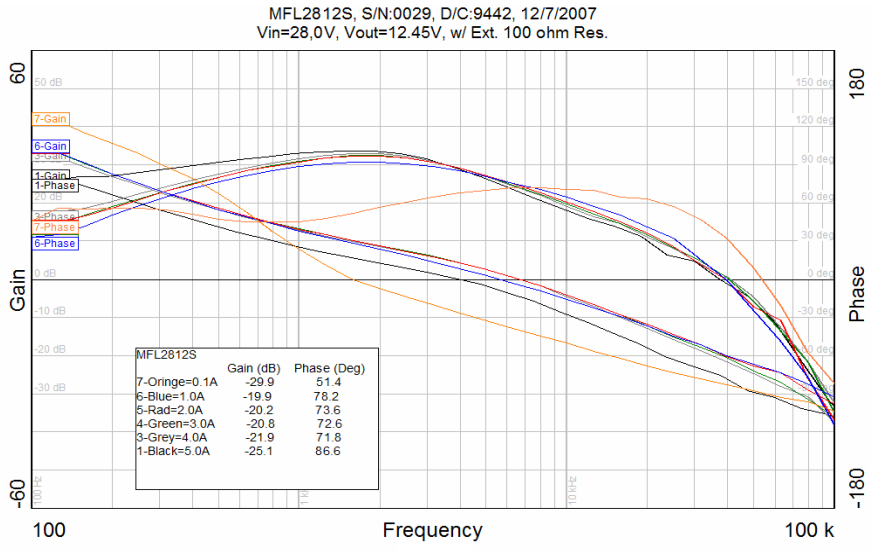
MFL2812S, S/N:0029, D/C:9442, 12/7/2007
Vin=28,0V, Vout=12.45V, w/ Ext. 100 ohm Res.
Gain
Phase
60
-60
180
-180
Frequency
100
100 k
MFL2812S
Gain (dB) Phase (Deg)
7-Oringe=0.1A -29.9 51.4
6-Blue=1.0A -19.9 78.2
5-Rad=2.0A -20.2 73.6
4-Green=3.0A -20.8 72.6
3-Grey=4.0A -21.9 71.8
1-Black=5.0A -25.1 86.6

(d)

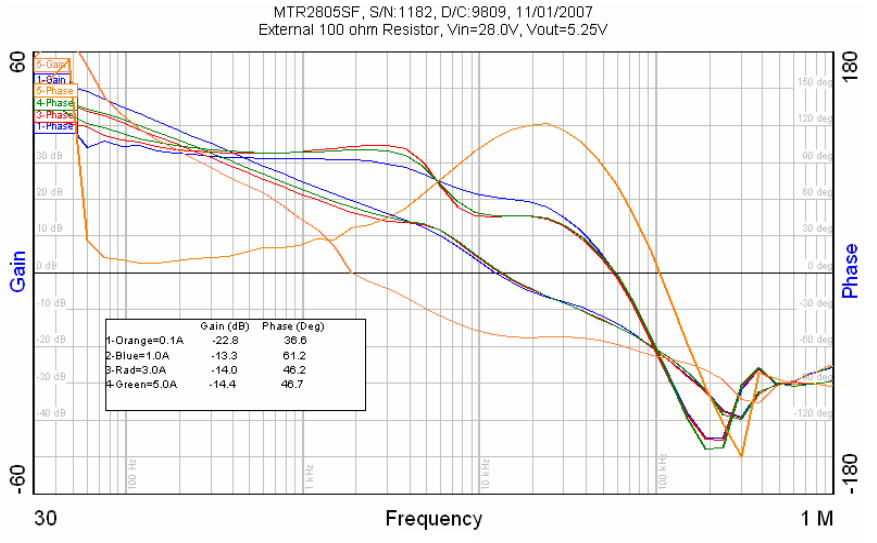
MTR2805SF, S/N:1182, D/C:9809, 11/01/2007
External 100 ohm Resistor, Vin=28.0V, Vout=5.25V
Gain
Phase
60
-60
180
-180
Frequency
30
1 M
Gain (dB) Phase (Deg)
1-Orange=0.1A -22.8 36.6
2-Blue=1.0A -13.3 61.2
3-Rad=3.0A -14.0 46.2
4-Green=5.0A -14.4 46.7

(e)

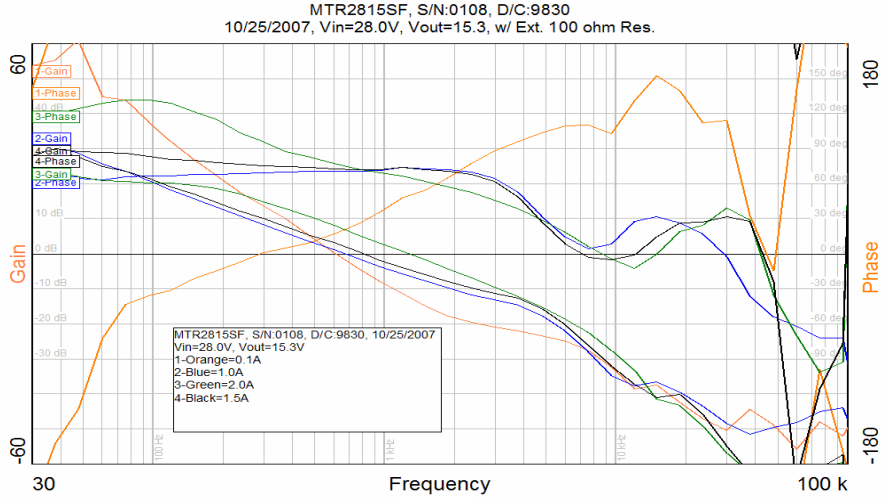
MTR2815SF, S/N:0108, D/C:9830
10/25/2007, Vin=28.0V, Vout=15.3, w/ Ext. 100 ohm Res.
Gain
Phase
60
-60
180
-180
Frequency
30
100 k
MTR2815SF, S/N:0108, D/C:9830, 10/25/2007
Vin=28.0V, Vout=15.3V
1-Orange=0.1A
2-Blue=1.0A
3-Green=2.0A
4-Black=1.5A

(f)

Appendix E: Test data of load current effect on gain/phase margins for eight DC/DC converters.

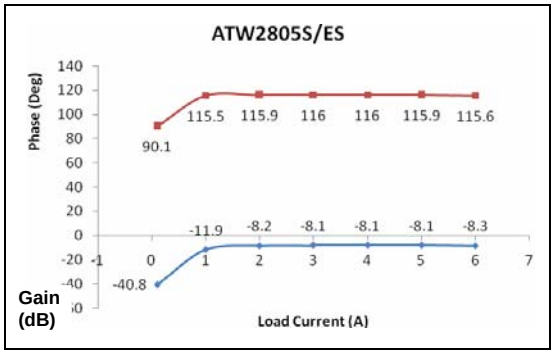

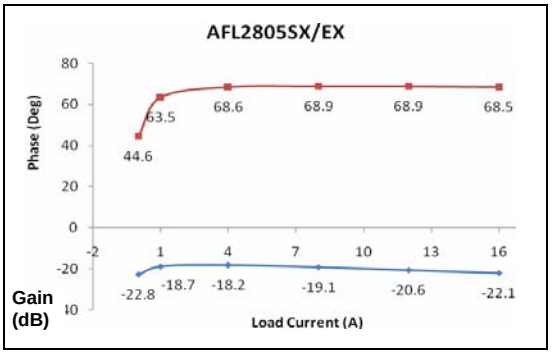

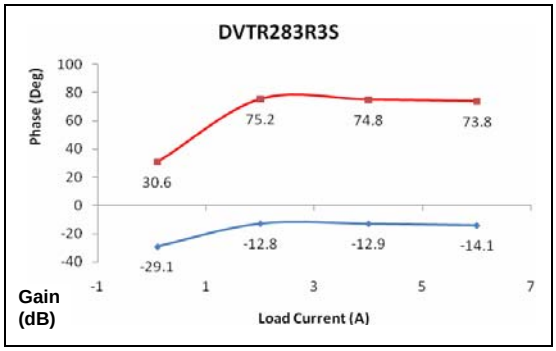

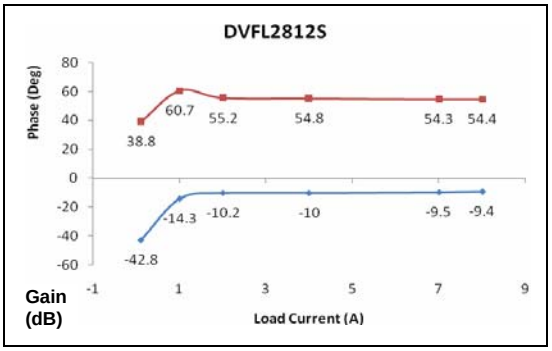

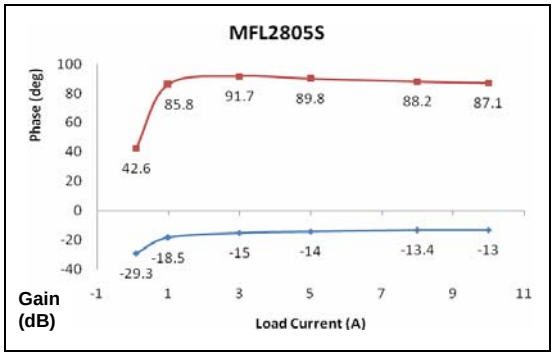

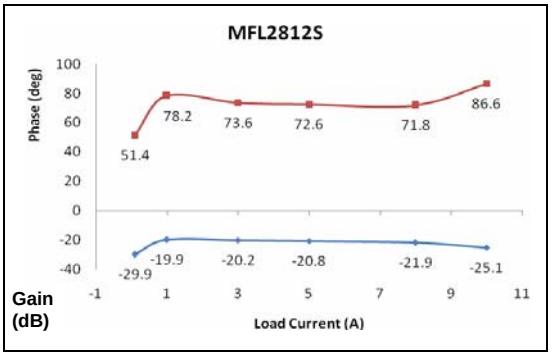

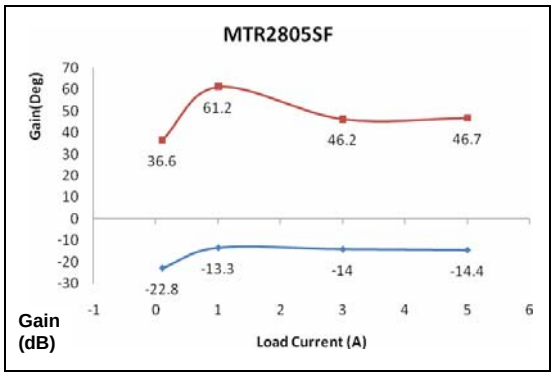

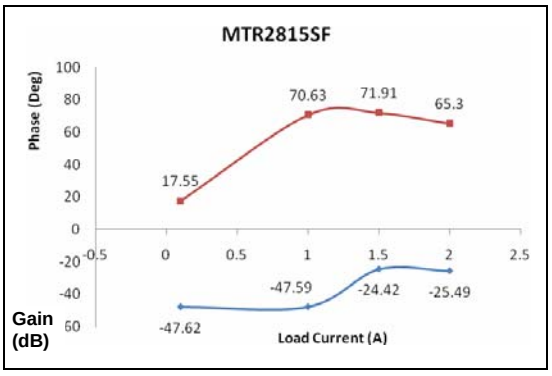

Appendix F: Temperature effects on gain margin at different power conditions for AFL2805S and DVFL2812S.

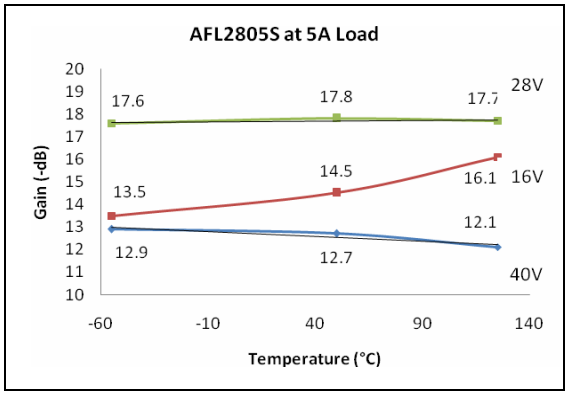

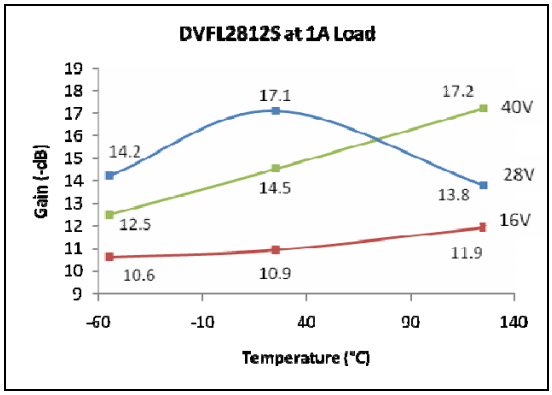

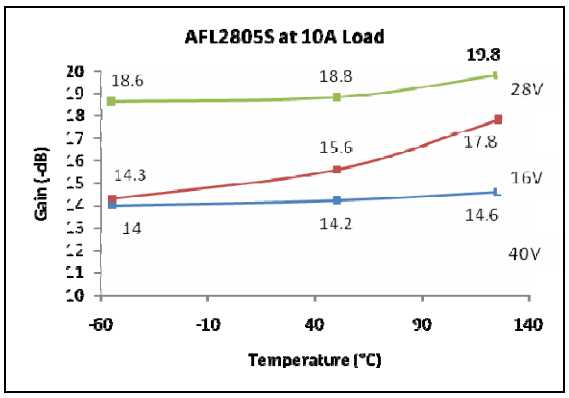

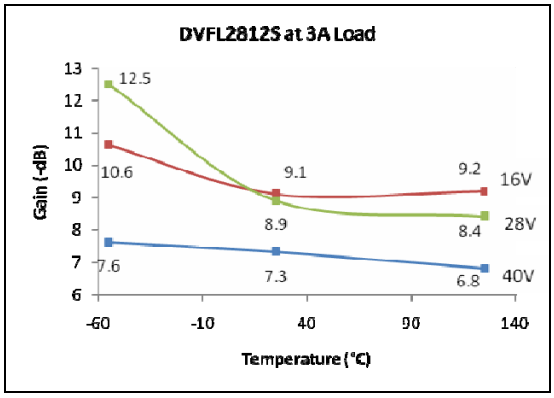

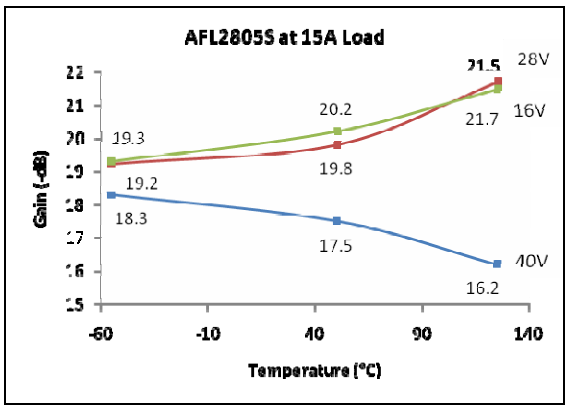

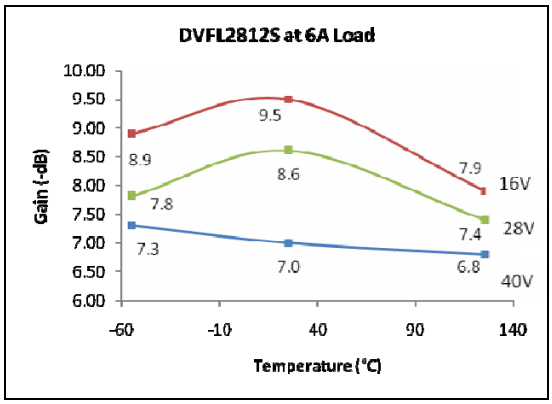

Appendix G: Temperature effects on phase margin at different power conditions for AFL2805S and DVFL2812S.

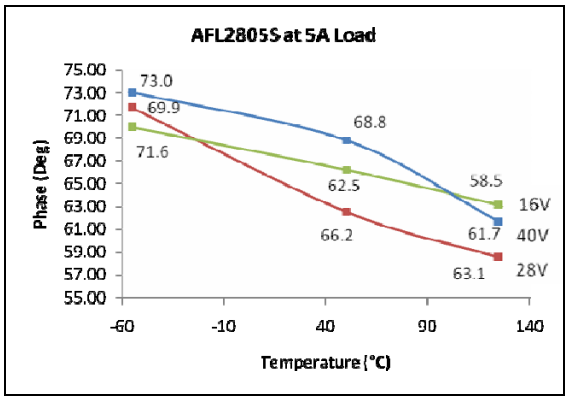

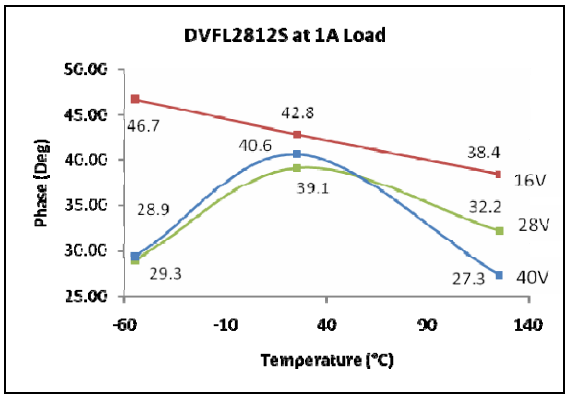

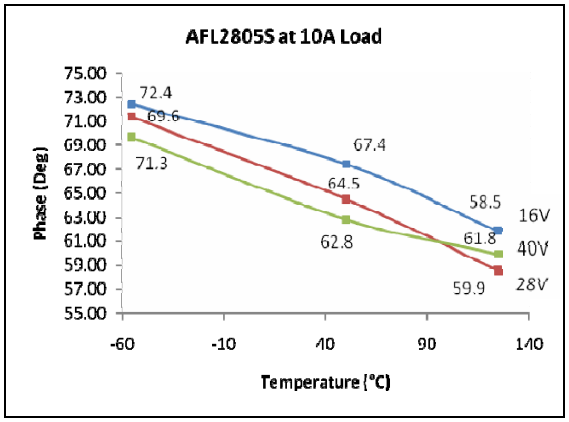

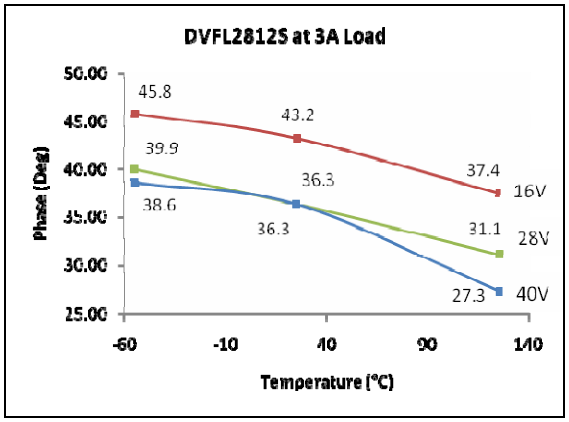

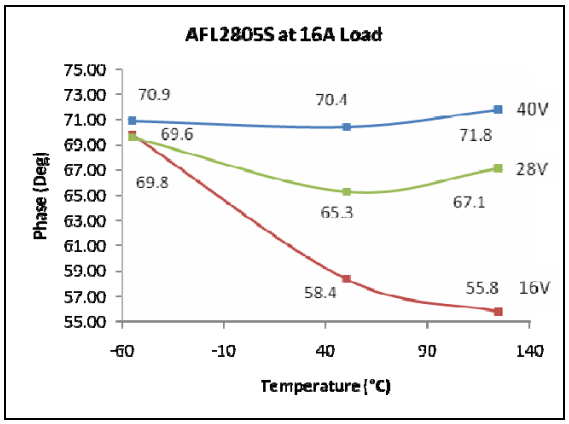

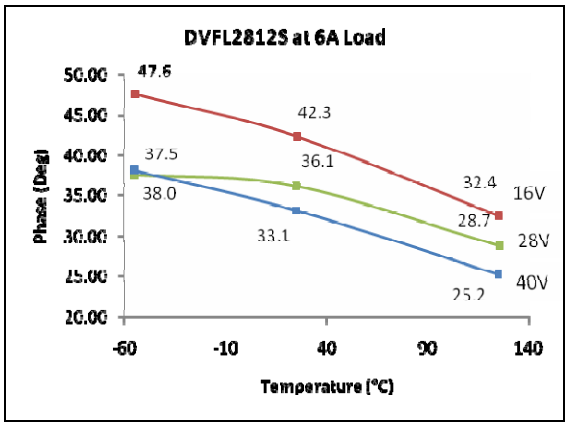

Appendix H: Feedback loop compensation netwok component variation effect on gain/phase margins for a QV24-5-25 open-frame module. (a) Bode plot, and (b) test data for Figures 21 (a) to (e).

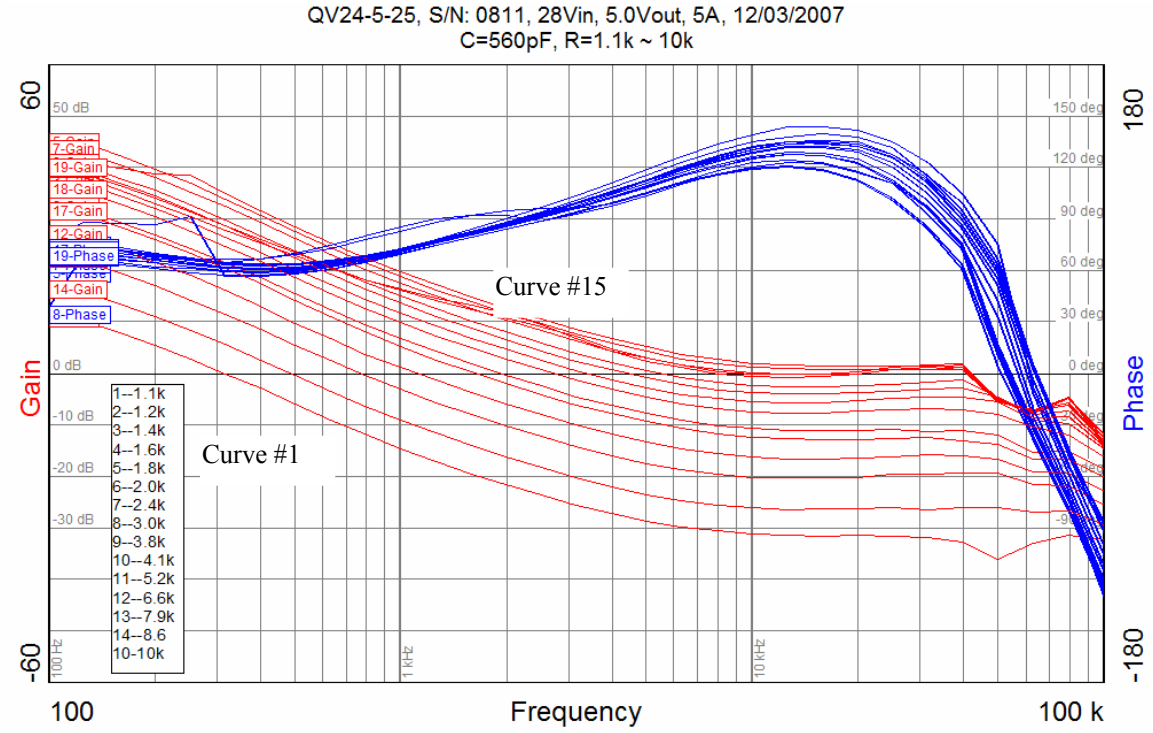

(a)

Curve #	R (kΩ)	Phase (deg)	Gain (dB)	Slope (-)	f_{cog} (kHz)	f_{cop} (kHz)
1	1.1	64.9	-33.4	1.41	0.314	61.7
2	1.2	63.1	-26.9	1.50	0.482	64.4
3	1.4	68.1	-21.6	1.40	0.768	64.6
4	1.6	74.9	-19.2	1.20	1.100	64.3
5	1.8	83.5	-16.7	1.10	1.620	63.8
6	2.0	86.4	-15.4	1.13	1.920	64.5
7	2.4	93.6	-10.3	0.99	2.700	62.0
8	3.0	99.6	-8.3	0.89	3.390	60.4
9	3.8	105.3	-7.4	0.79	4.360	58.5
10	4.1	111.0	-6.6	0.65	5.460	57.2
11	5.2	115.9	-5.8	0.50	7.920	53.9
12	6.6	125.7	-6.1	0.08	10.420	54.6
13	7.5	53.6	-5.9	0.02	20.000	52.7
14	8.6	50.5	-5.6	3.20	41.500	51.3
15	10.0	121.5	-5.7	0.30	9.370	53.3

Note: f_{cog}, and f_{cop} are crossover frequencies of the gain and phase, respectively.

(b)

Appendix I: Raw data for Figure 22 (b), (d), and (f); and for Figure 23 (a) to (f). Correlation between gain/phase crossover frequencies and channel power frequencies for oscillation identifiication and early detection using spectral analysis.

AFL2805S

*Temp (°C)	*Bode Plot No.	*Spectrum No.	Channel Power (dBm)	Phase Cross Frequency (kHz)	Ch. Power Frequency (kHz)	Gain Margin (dB)	Phase Margin (Deg)
30	20	42	75.9	113.8	96.6	-27.3	44.9
16	21	43	72.9	117.6	103.1	-25.1	44.0
-3	22	46	85.1	124.7	117.4	-14.9	45.1
-20	23	47	81.6	135.3	135.7	-24.6	46.7
-39	24	45	84.9	-	-	-24.1	48.5
-45	27	39	85.5	98.9	94.6	-17.6	69.9
-48	43	52	47.9	148.8	146.5	-	-

Columns with * are for test reference only.

QV24-5-25

*Bode Plot No.	Channel Power (dBm)	Channel Power Frequency (kHz)	Phase Crossover Frequency(kHz)	Gain Margin (dB)	Phase Margin (deg)
01	-57.5	64.5	61.7	-33.4	64.9
14	-57.4	65.3	64.5	-26.9	63.1
13	-57.3	66.2	64.5	-21.6	68.1
12	-57.0	66.8	64.0	-19.2	74.9
17	-56.8	64.4	64.0	-16.4	82.3
02	-56.5	64.9	64.5	-15.4	86.4
18	-56.0	65.7	62.1	-10.3	93.6
03	-55.3	64.5	60.3	-8.3	99.6
19	-54.8	63.8	58.5	-7.4	105.3
04	-54.4	62.9	57.2	-6.6	111.0
24	-53.6	61.1	59.3	-7.1	107.6
05	-53.4	56.6	54.6	-5.9	117.6
06	-52.2	55.5	51.0	-5.6	120.0
07	-51.5	58.4	54.6	-6.1	125.7
08	-50.4	58.6	53.8	-5.8	125.9
09	-49.3	56.6	53.4	-5.8	121.5
21	-48.3	57.7	54.2	-5.6	113.8
22	-47.2	58.0	53.8	-5.7	110.4

Column with * is for test reference only.

MFL2812S

*Bode Plot No:	Channel Power (dBm)	Channel Power Frequency (kHz)	Phase Crossover Frequency (kHz)	Gain Margin (dB)	Phase Margin (Deg)
24	-71.7	34.5	34.7	-20.4	70.6
27	-63.2	30.0	29.4	-11.4	74.3
28	-32.2	31.2	30.8	-11.0	78.9
29	-68.6	38.1	40.9	-26.7	86.2

Column with * is for test reference only.

Appendix J: Sample power spectra at different operating conditions for input voltage noise of MFL2812S. Figures (a), (b) and (c) show early stages of oscillation, and (d) point of oscillation.

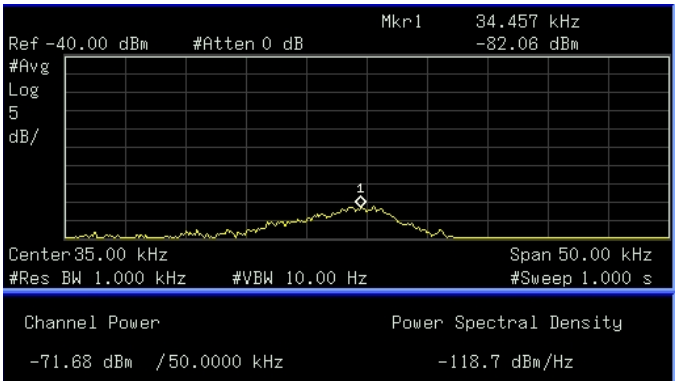

(a) Vin = 24.3V, Iout = 3.0A, Channel Power Freq. = 34 kHz

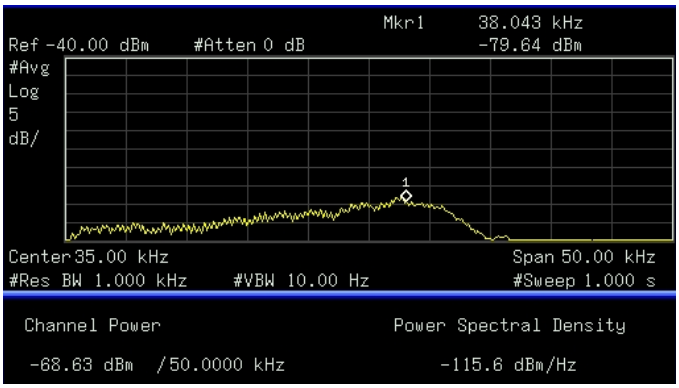

(b) Vin = 28.0V, Iout = 5.0A, Channel Power Freq. = 38 kHz

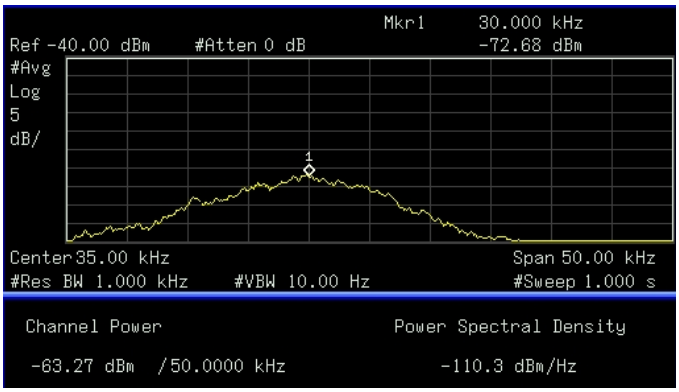

(c) Vin = 21.9V, Iout = 3.0A, Channel Power Freq. = 30 kHz

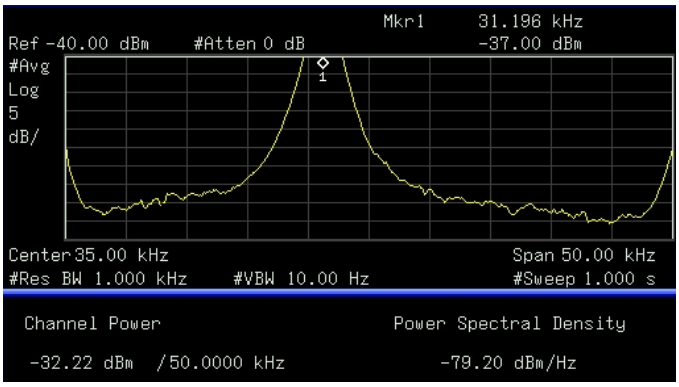

(d) Vin = 20.9V, Iout = 3.0A, Channel Power Freq. = 31 kHz

REPORT DOCUMENTATION PAGE

Form Approved
OMB No. 0704-0188

1. REPORT DATE *(DD-MM-YYYY)*	2. REPORT TYPE	3. DATES COVERED *(From - To)*
22-07-2008	Contractor Report (CR)	March 2007- January 2008

4. TITLE AND SUBTITLE

DC/DC Converter Stability Testing Study

5a. CONTRACT NUMBER
ESES 260

5b. GRANT NUMBER
GSS-05-S-246

5c. PROGRAM ELEMENT NUMBER
n/a

6. AUTHOR(S)

Bright L. Wang

5d. PROJECT NUMBER
n/a

5e. TASK NUMBER
n/a

5f. WORK UNIT NUMBER
n/a

7. PERFORMING ORGANIZATION NAME(S) AND ADDRESS(ES)

Perot Systems Government Services (PSGS)
7404 Executive Place, Suite 500, Seabrook MD 20706 under contract to
NASA Goddard Space Flight Center
Greenbelt MD 20771

8. PERFORMING ORGANIZATION REPORT NUMBER

9. SPONSORING/MONITORING AGENCY NAME(S) AND ADDRESS(ES)

National Aeronautics and Space Administration
Goddard Space Flight Center
Greenbelt MD 20771

10. SPONSORING/MONITOR'S ACRONYM(S)
NASA

11. SPONSORING/MONITORING REPORT NUMBER
CR-2008-214163

12. DISTRIBUTION/AVAILABILITY STATEMENT

Unclassified - Unlimited
NASA Center for AeroSpace Information (301) 621-0390

13. SUPPLEMENTARY NOTES

Bright Wang: Perot Systems Government Services (PSGS), Seabrook, MD

14. ABSTRACT

This report presents study results on hybrid DC/DC converter stability testing methods. An input impedance measurement method and a gain/phase margin mesurement method were evaluated to be effective to determine front-end oscillation and feedback loop oscillation. In particular, certain channel power levels of conveter input noises have been found to have high degree correlation with the gain/phase margins. It becomes a potential new method to evaluate stability levels of all type of DC/DC converters by utilizing the spectral analysis on converter input noises.

Jelila S. Mohammed, COTR (CM); An electronic version of this report can be found at http://nepp.gsfc.nasa.gov.

15. SUBJECT TERMS

Hybrid DC/DC converter, Input impedance, Gain and Phase margin, Stability, Spectral analysis,

16. SECURITY CLASSIFICATION OF:			17. LIMITATION OF ABSTRACT	18. NUMBER OF PAGES	19b. NAME OF RESPONSIBLE PERSON
a. REPORT	b. ABSTRACT	c. THIS PAGE			Jelila S. Mohammed (jelila.s.mohammed@nasa.go
U	U	U	UU	39	19b. TELEPHONE NUMBER *(Include area code)* (301) 286-0390